Catena 170 (2018) 335–355

Contents lists available at ScienceDirect

Catena

journal homepage: www.elsevier.com/locate/catena

Pedogenic and microbial interrelations to regional climate and local topography: New insights from a climate gradient (arid to humid) along the Coastal Cordillera of Chile

Nadine Bernhard[a,*,1], Lisa-Marie Moskwa[b,1], Karsten Schmidt[a], Ralf A. Oeser[c], Felipe Aburto[d], Maaike Y. Bader[e], Karen Baumann[f], Friedhelm von Blanckenburg[c,g], Jens Boy[h], Liesbeth van den Brink[i], Emanuel Brucker[j], Burkhard Büdel[k], Rafaella Canessa[e], Michaela A. Dippold[l], Todd A. Ehlers[m], Juan P. Fuentes[n], Roberto Godoy[o], Patrick Jung[k], Ulf Karsten[p], Moritz Köster[l], Yakov Kuzyakov[q], Peter Leinweber[f], Harald Neidhardt[r], Francisco Matus[s], Carsten W. Mueller[t], Yvonne Oelmann[r], Rómulo Oses[u,v], Pablo Osses[w], Leandro Paulino[x], Elena Samolov[p], Mirjam Schaller[m], Manuel Schmid[m], Sandra Spielvogel[y], Marie Spohn[j], Svenja Stock[q], Nicole Stroncik[c], Katja Tielbörger[i], Kirstin Übernickel[m], Thomas Scholten[a], Oscar Seguel[z], Dirk Wagner[b,aa], Peter Kühn[a]

[a] University of Tübingen, Department of Geosciences, Soil Science and Geomorphology, Rümelinstraße 19–23, D-72070 Tübingen, Germany
[b] GFZ German Research Centre for Geosciences, Section 5.3 Geomicrobiology, Telegrafenberg, D-14473 Potsdam, Germany
[c] GFZ German Research Centre for Geosciences, Section 3.3 Earth Surface Geochemistry, Telegrafenberg, D-14473 Potsdam, Germany
[d] Universidad de Concepción, Departamento de Silvicultura, Facultad de Ciencias Forestales, Victoria 631, Concepción, Chile
[e] University of Marburg, Faculty of Geography, Plant Ecological Biogeography, Deutschhausstrasse 10, D-35032 Marburg, Germany
[f] University of Rostock, Faculty of Agricultural and Environmental Sciences, Soil Science, Justus-von-Liebig-Weg 6, D-18059 Rostock, Germany
[g] Freie Universität Berlin, Institute of Geological Science, Malteserstr. 74–100, Building N, D-12249 Berlin, Germany
[h] Leibniz University of Hannover, Institute of Soil Science, Herrenhäuser Straße 2, D-30419 Hannover, Germany
[i] University of Tübingen, Plant Ecology, Auf der Morgenstelle 5, D-72076 Tübingen, Germany
[j] University of Bayreuth, Institute of Soil Ecology, Dr.-Hans-Frisch-Straße 1–3, D-95448 Bayreuth, Germany
[k] Technical University Kaiserslautern, Department Plant Ecology and Systematics, Institute of Biology, Erwin-Schrödinger-Str. 13, D-67663 Kaiserslautern, Germany
[l] Georg-August-University of Göttingen, Biogeochemistry of Agroecosystems, Büsgenweg 2, D-37077 Göttingen, Germany
[m] University of Tübingen, Department of Geosciences, Wilhelmstraße 56, D-72074 Tübingen, Germany
[n] Universidad de Chile, Facultad de Ciencias Forestales y de la Conservación de la Naturaleza, Av. Santa Rosa, 11315 La Pintana, Santiago, Chile
[o] Universidad Austral de Chile, Instituto de Ciencias Ambientales y Evolutivas, Avenida Eduardo Morales Miranda, Campus Isla Teja, 5090000 Valdivia, Chile
[p] University of Rostock, Institute of Biological Sciences, Applied Ecology and Phycology, Albert-Einstein-Strasse 3, D-18059 Rostock, Germany
[q] Georg-August-University of Göttingen, Soil Science of Temperate Ecosystems, Büsgenweg 2, D-37077 Göttingen, Germany
[r] University of Tübingen, Geoecology, Rümelinstraße 19–23, D-72070 Tübingen, Germany
[s] Universidad de La Frontera, Departamento de Ciencias Químicas y Recursos Naturales, Scientific and Technological Bioresource Nucleus (BIOREN-UFRO), Temuco, Chile
[t] Technical University of Munich, Research Department Ecology and Ecosystem Management, Freising, Germany
[u] Centro de Estudios Avanzados en Zonas Aridas (CEAZA), Raúl Britán #1305, Campus Andrés Bello Universidad de La Serena, La Serena, Chile
[v] Universidad de Atacama, CRIDESAT, Copayapu 484, Copiapó, Chile
[w] Pontificia Universidad Católica de Chile, Instituto de Geografía, Vicuña Mackenna, 4860 Macul, Santiago, Chile

Abbreviations: AZ, Pan de Azúcar; SG, Santa Gracia; LC, La Campana; NA, Nahuelbuta; MAT, mean annual temperature; MAP, mean annual precipitation; PET, potential evapotranspiration; LAI, leaf area index; CAM, Crassulacean acid metabolism; BD, bulk density; TOC, total organic carbon; BS, base saturation; CEC_{eff}, effective cation exchange capacity; Al_{ex}, exchangeable aluminum

* Corresponding author.
E-mail addresses: nadine.bernhard@uni-tuebingen.de (N. Bernhard), lmmoskwa@gfz-potsdam.de (L.-M. Moskwa), karsten.schmidt@uni-tuebingen.de (K. Schmidt), oeser@gfz-potsdam.de (R.A. Oeser), feaburto@udec.cl (F. Aburto), maaike.bader@uni-marburg.de (M.Y. Bader), karen.baumann@uni-rostock.de (K. Baumann), fvb@gfz-potsdam.de (F. von Blanckenburg), boy@ifbk.uni-hannover.de (J. Boy), liesbeth.vandenbrink@uni-tuebingen.de (L. van den Brink), Emanuel.brucker@uni-bayreuth.de (E. Brucker), buedel@rhrk.uni-kl.de (B. Büdel), rcanessa@uni-marburg.de (R. Canessa), dippold@gwdg.de (M.A. Dippold), todd.ehlers@uni-tuebingen.de (T.A. Ehlers), jufuente@uchile.cl (J.P. Fuentes), rgodoy@uach.cl (R. Godoy), ulf.karsten@uni-rostock.de (U. Karsten), mkoester@gwdg.de (M. Köster), kuzyakov@gwdg.de (Y. Kuzyakov), peter.leinweber@uni-rostock.de (P. Leinweber), harald.neidhardt@uni-tuebingen.de (H. Neidhardt), francisco.matus@ufrontera.cl (F. Matus), carsten.mueller@wzw.tum.de (C.W. Mueller), yvonne.oelmann@uni-tuebingen.de (Y. Oelmann), romulo.oses@ceaza.cl, romulo.oses@uda.cl (R. Oses), posses@uc.cl (P. Osses), lpaulino@udec.cl (L. Paulino), elena.samolov@uni-rostock.de (E. Samolov), mirjam.schaller@uni-tuebingen.de (M. Schaller), manuel.schmid@uni-tuebingen.de (M. Schmid), s.spielvogel@soils.uni-kiel.de (S. Spielvogel), marie.spohn@uni-bayreuth.de (M. Spohn), svenja.stock@forst.uni-goettingen.de (S. Stock), stroncik@gfz-potsdam.de (N. Stroncik), katja.tielboerger@uni-tuebingen.de (K. Tielbörger), kirstin.uebernickel@uni-tuebingen.de (K. Übernickel), thomas.scholten@uni-tuebingen.de (T. Scholten), oseguel@uchile.cl (O. Seguel), dirk.wagner@gfz-potsdam.de (D. Wagner), peter.kuehn@uni-tuebingen.de (P. Kühn).
[1] These authors contributed equally to this work.

https://doi.org/10.1016/j.catena.2018.06.018

[x] Universidad de Concepción, Departamento de Suelos y Recursos Naturales, Facultad de Agronomía, Avda. Vicente Méndez 595, Chillán, Chile
[y] Christian-Albrechts-University of Kiel, Institute of Soil Science, Hermann-Rodewald-Straße 2, D-24118 Kiel, Germany
[z] Universidad de Chile, Facultad de Ciencias Agronómicas, Av. Santa Rosa #11315, 8820808 La Pintana, Santiago, Chile
[aa] University of Potsdam, Institute of Earth and Environmental Sciences, D-14476 Potsdam, Germany

ARTICLE INFO

Keywords:
Climate
Topography
Soil texture
Total organic carbon
Carbon isotope ratio ($\delta^{13}C_{TOC}$)
Microbial abundance

ABSTRACT

The effects of climate and topography on soil physico-chemical and microbial parameters were studied along an extensive latitudinal climate gradient in the Coastal Cordillera of Chile (26°–38°S). The study sites encompass arid (Pan de Azúcar), semiarid (Santa Gracia), mediterranean (La Campana) and humid (Nahuelbuta) climates and vegetation, ranging from arid desert, dominated by biological soil crusts (biocrusts), semiarid shrubland and mediterranean sclerophyllous forest, where biocrusts are present but do have a seasonal pattern to temperate-mixed forest, where biocrusts only occur as an early pioneering development stage after disturbance. All soils originate from granitic parent materials and show very strong differences in pedogenesis intensity and soil depth.

Most of the investigated physical, chemical and microbiological soil properties showed distinct trends along the climate gradient. Further, abrupt changes between the arid northernmost study site and the other semi-arid to humid sites can be shown, which indicate non-linearity and thresholds along the climate gradient. Clay and total organic carbon contents (TOC) as well as Ah horizons and solum depths increased from arid to humid climates, whereas bulk density (BD), pH values and base saturation (BS) decreased. These properties demonstrate the accumulation of organic matter, clay formation and element leaching as key-pedogenic processes with increasing humidity. However, the soils in the northern arid climate do not follow this overall latitudinal trend, because texture and BD are largely controlled by aeolian input of dust and sea salts spray followed by the formation of secondary evaporate minerals. Total soil DNA concentrations and TOC increased from arid to humid sites, while areal coverage by biocrusts exhibited an opposite trend. Relative bacterial and archaeal abundances were lower in the arid site, but for the other sites the local variability exceeds the variability along the climate gradient. Differences in soil properties between topographic positions were most pronounced at the study sites with the mediterranean and humid climate, whereas microbial abundances were independent on topography across all study sites. In general, the regional climate is the strongest controlling factor for pedogenesis and microbial parameters in soils developed from the same parent material. Topographic position along individual slopes of limited length augmented this effect only under humid conditions, where water erosion likely relocated particles and elements downward. The change from alkaline to neutral soil pH between the arid and the semi-arid site coincided with qualitative differences in soil formation as well as microbial habitats. This also reflects non-linear relationships of pedogenic and microbial processes in soils depending on climate with a sharp threshold between arid and semi-arid conditions. Therefore, the soils on the transition between arid and semi-arid conditions are especially sensitive and may be well used as indicators of long and medium-term climate changes. Concluding, the unique latitudinal precipitation gradient in the Coastal Cordillera of Chile is predestined to investigate the effects of the main soil forming factor – climate – on pedogenic processes.

1. Introduction

Soil forms at the interface between the atmosphere and lithosphere sustaining Earth's life and biogeochemical cycles (Amundson et al., 2007). Excluding anthropogenic effects, soils and their properties are commonly regarded as forming from interactions between five factors including: climate, biota, topography, parent material and time (e.g. Dokuchaiev, see Glinka, 1927; Hilgard, 1914; Jenny, 1994). Climate has a strong effect on soil properties via biological and hydrological processes, as the changing water flow, vegetation and soil biological activity affects soil physical and chemical properties, including BD, soil organic matter, clay formation, pH value and the degree of leaching or accumulation of base cations and pedogenesis in general (Bojko and Kabala, 2017; Jenny, 1994; Lin, 2010; Pastalkova et al., 2001; Smith et al., 2002).

Previous studies on latitudinal and elevational soil-climate gradients with similar parent materials (including granites, loess, basalts, paragneiss) demonstrated that increasing precipitation and decreasing temperature result in a decrease of silt contents, soil pH and BS, whereas TOC, acidity and exchangeable aluminum (Al_{ex}), electrical conductivity and clay contents increase (Bardelli et al., 2017; Bojko and Kabala, 2016; Khomo et al., 2011; Khormali et al., 2012; Raheb et al., 2017; Smith et al., 2002; Xu et al., 2014). Specific thresholds for the occurrence of shifts in these properties, like a certain elevation, e.g. > 1000 m a.s.l. or a mean annual precipitation (MAP) of 1400 mm were suggested (Bojko and Kabala, 2017; Chadwick et al., 2003). According to Slessarev et al. (2016), the pH value has a threshold with a steep transition from alkaline to acidic when MAP exceeds potential evapotranspiration (PET). Regarding the soil microflora, microorganisms are highly responsive to their environment and the composition of microbial communities is shaped by a wide range of soil properties. For example, several studies highlighted the influence of pH (Lauber et al., 2009), particle size (Sessitsch et al., 2001; Wagner et al., 1999), organic carbon content (Fierer et al., 2007; Goldfarb et al., 2011; Zhou et al., 2002) and nutrient availability (Fierer et al., 2003) on microorganisms. In general, microbial abundances tend to be lower under arid climate conditions, increase with increasing precipitation (Bachar et al., 2010; Fierer et al., 2012; Ollivier et al., 2014) and decrease with soil depth (Agnelli et al., 2004; Fierer et al., 2003; Goberna et al., 2005; Schulze-Makuch et al., 2018; Will et al., 2010). The previous studies show that the study of pedogenic characteristics and microbial abundances along latitudinal gradients is a promising approach to explore the interactions between climate effects on soils and microorganisms, and to identify the thresholds involved.

In addition to climate, the topographic position of soils is regarded as an essential factor in soil formation ever since Milne (1935) published the concept of a catena. A catena describes soils along a landscape sequence, where soil properties change gradually depending on geological, geomorphic, atmospheric, or biological processes with upslope mobilization, downslope redistribution and transfer of solutes, colloids and particles (Sommer and Schlichting, 1997; Wysocki and Zanner, 2006). Bojko and Kabala (2016) reported finer soil textures and higher contents of base cations downslope as a result of the selective transport of material along the slope for soil developed from granitic

parent material within the Karkonosze mountains in Poland. The rates and mechanisms of hillslope processes, however, change with climate conditions. Khomo et al. (2011) described an increasing intensity of clay redistribution on hillslopes from top to foot slope position with increasing precipitation, influencing other soil properties as a consequence of the differing clay contents. Biota contribute also to slope-dependent transport of soil (Amundson et al., 2015) and soil fertility can be related to topography as well (Scholten et al., 2017). However, a study relating soil and microbial characteristics and their interrelations to slope-dependent transport processes is still missing.

Another factor of local topography, the slope aspect (e.g. north-facing vs. south-facing), affects the local microclimate with lower soil temperatures and higher soil moisture on sun-averted slopes (Barbosa et al., 2015; Carletti et al., 2009; Egli et al., 2006; Zhao and Li, 2017). Aspect can influence both physico-chemical and microbial parameters. Higher soil organic matter contents (Barbosa et al., 2015; Carletti et al., 2009) and more intense leaching and acidification on the moister slope were detected (Zhao and Li, 2017). However, Egli et al. (2006) did not find such differences in soil organic matter between slope exposures in moderate to high alpine climate zones. Gómez-Brandón et al. (2017) detected higher microbial abundances in combination with higher microbial activity on a moister sun-adverted slope, whereas Zhao and Li (2017) detected lower microbial activity on the sun-averted slope, most likely due to the lower temperatures. These diverging case studies show that further research is necessary to detect the general role of slope aspect induced microclimate effects on soil organic matter and microbial properties.

In the Coastal Cordillera of Chile, a broad climatic and ecologic gradient can be found due to the large latitudinal extent (Fig. 1). The proximity to the Pacific Ocean, the effects of the Humboldt Current and the Pacific High-Pressure Zone lead to a climate varying from extreme aridity in the north (e.g. Atacama Desert), to a mediterranean climate in central Chile, and finally to a colder and rainier climate in the south (Garreaud et al., 2009; Pizarro et al., 2012). In accordance with the climate, the vegetation types range from very sparse higher desert vegetation, but abundant cryptogamic cover (biological soil crusts or biocrusts) as associations of microorganisms and soil particles in the top millimeters of the soil, via semi-arid open shrubland and mediterranean dry forest to temperate mixed broadleaved-coniferous forest. Concordantly, characteristic soils range from salt-enriched soils and undeveloped soils like Leptosols in the dry north to Cambisols, Lixisols, Fluvisols, Luvisols, Acrisols, Umbrisols and Andosols in the south of Chile (Casanova et al., 2013). The broad latitudinal climate gradient of Chile now offers the possibility to differentiate in our study between climatic and local topographic effects on soils developed from similar parent material.

In this study, we evaluate the hypotheses that: (1) Soil formation and microbial abundances will increase from the arid to the humid

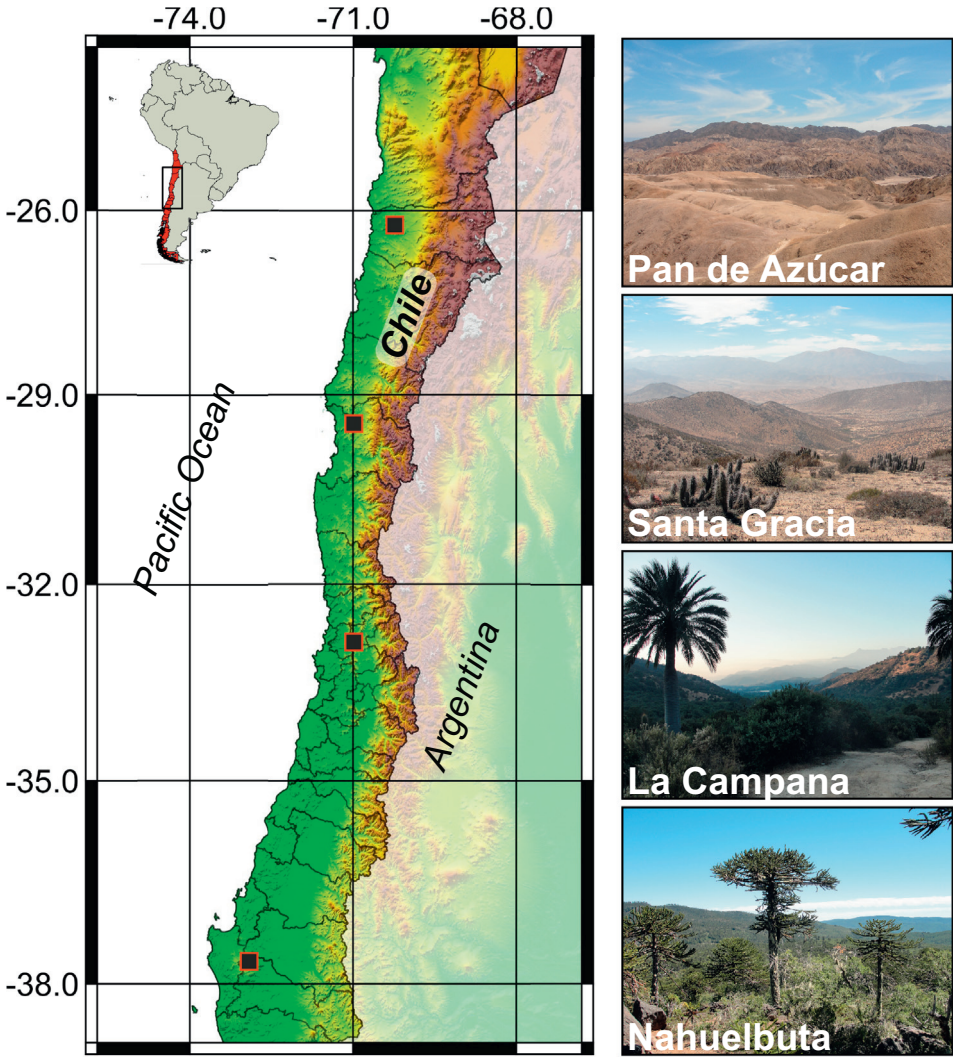

Fig. 1. Location of the four primary EarthShape study areas (squares, from north to south): Pan de Azúcar, Santa Gracia, La Campana, and Nahuelbuta (different colors represent elevation bands).

climate (regional scale). However, potential non-linearity and thresholds occur along the gradient for specific soil properties. (2) A local gradient of soil properties along the catena (local hillslope scale) due to changes of moisture and downslope movement of solutes and soil will be present. This trend is minor in comparison to the regional scale as this steep climate gradient overprints local heterogeneity. (3) Soil properties and microbial abundances are affected by aspect. Our investigations along the Costal Cordillera of Chile allow us to identify regional and local trends and interrogate whether local variability of physico-chemical and microbial parameters exceed the climate gradient, or if climate overprints local heterogeneity.

The research presented in this paper is part of the German-Chilean priority research program EarthShape (www.earthshape.net). EarthShape (Earth Surface Shaping by Biota) is a large research network studying the role of microorganisms, animals and higher plants for shaping and developing the Earth's surface over time scales from the present-day to the distant geologic past. It includes investigations into the influence of climate, vegetation and topography on weathering, pedogenesis and microbial abundances. A companion publication (Oeser et al., 2018) describes the architecture of the weathering zone, the degree and rate of rock weathering, denudation rates and microbial abundances of bacteria and archaea in the saprolite. With these two papers, we also provide the basic critical zone background data that will serve as basis for future studies employing other field and laboratory techniques in EarthShape that aim to decipher the role of biota in Earth surface shaping along the EarthShape gradient.

2. Material and methods

2.1. Environmental settings of the study sites

The four primary study sites of EarthShape (Fig. 1) are located in the Coastal Cordillera of Chile from 26°S to 38°S. The study sites are situated within the nature protection sites Pan de Azúcar National Park (AZ), Santa Gracia Natural Reserve (SG), La Campana National Park (LC) and Nahuelbuta National Park (NA). The Coastal Cordillera consists mostly of early Permian to late Triassic igneous rocks (Hervé et al., 2007; Pankhurst and Hervé, 2007), mainly composed of hornblende-biotite gabbros, diorites, tonalities/granodiorites and minor granites (Parada et al., 2007). Along the studied gradient, the lithology comprises granitoid parent material only, allowing to keep this factor of soil formation rather constant. In detail, the bedrock samples from AZ, LC and NA are granites, granodiorites, and tonalites, respectively. SG bedrock is dioritic (Oeser et al., 2018). The tectonic uplift maintains topography with generally V-shaped valleys. The study sites were not glaciated as the most northern limit of the last glaciation in the Coastal Cordillera was 40°S (Hulton et al., 2002).

The climate in Chile is strongly influenced by the South Pacific anticyclone, which produces the characteristic clear skies in the north of Chile and controls floods and droughts (Muñoz et al., 2007). The monthly rainfall distribution patterns are similar in all sites, where most of the rainfall occurs in the austral winter months May to August. The mean annual temperature (MAT) decreases from north (AZ, 16.8 °C) to south (NA, 6.6 °C, Table 1). The MAP increases from north to south in the study sites and ranges from 12 mm in AZ to 1469 mm in NA (Table 1). Even though the MAP increases gradually with latitude from north to south, rainfall intensity does not change much (Pizarro et al., 2012). This leads to different soil moisture regimes in the study sites from north to south: aridic – xeric-udic (Gardi et al., 2015). AZ is located in the northern zone (~26°S), in the Atacama Desert, with almost no rainfall and mostly endorheic water resources. SG is located in the semi-arid zone (~29°S) with mostly winter rainfall and substantial annual variation in the precipitation quantities (Table 1) and LC lies within the central zone (~32°S) with rainfall concentrated during the cold winter season, as it is typical for mediterranean climate. NA is located in the cold and humid zone (~38°S; Muñoz et al., 2007). The duration of this climate pattern is supposed to have persisted since the late Pliocene for northern Chile as evidenced by paleoclimate modeling (Jungers et al., 2013; Mutz et al., 2018), geological and marine records. Thus, this region should reflect long-term impact of climate on soils (Ewing et al., 2006). In accordance with the climate, the vegetation types in the study sites range from very sparse higher plant desert vegetation in the north, where biocrust soil coverage can reach as much as 40% of the area (which is named then biocrust-dominated desert vegetation) (Table S6, Bernhard et al., 2018) to semi-desert open shrubland to mediterranean dry forest and to temperate mixed broadleaved-coniferous forest in the south.

2.2. Soil sampling and classification

In each study site, one catena was established with three south-facing soil profiles on different hillslope positions (upper, mid and lower slope), and an additional profile on the north-facing mid slope. For each of the soil profiles, one additional shallow replicate profile (plot replicates) was established up to 40 cm depth. This enabled us to analyze regional variations of physico-chemical and microbial soil properties between the four study sites along the climate gradient and further, the local variations between the topographic positions along the hillslopes (upper vs. mid vs. lower slope), as well as influences of aspects (north- vs. south-facing slopes due to their highest insolation difference).

Soils were described and classified according to Food and Agriculture Organization of the United Nations (FAO, 2006) and IUSS Working Group WRB (2015). Sampling was carried out horizon-wise and per depth increment 0–5, 5–10, 10–20 and 20–40 cm, and further down to the weathered rock or saprolite in 20 cm steps. Bulk samples were taken from the soil genetic horizons and depth increments. Additional volumetric samples from the depth increments were sampled as triplicates by using 100 cm^3 steel cylinders for BD. Separate samples were collected for DNA-based methods under sterile conditions and were stored at −20 °C until further processing.

2.3. Physical and chemical soil analysis

All bulk samples were, if not indicated differently, air dried and sieved (< 2 mm) before the following analyses.

The BD was gravimetrically (samples dried at 105 °C) determined

Table 1
Location of the soil pits and climate characteristics of the study sites Pan de Azúcar (AZ), Santa Gracia (SG), La Campana (LC) and Nahuelbuta (NA). MAT = mean annual temperature, MAP = mean annual precipitation.

Location	Longitude	Latitude	MAT[a] [°C]	MAP[a] [mm]	Elevation [m a.s.l.]	Climate classification[b,c]
AZ	−70.549	−26.110	16.8	12	329–351	Arid
SG	−71.166	−29.757	13.7	66	642–720	Semiarid
LC	−71.063	−32.955	14.1	367	708–732	Mediterranean
NA	−73.013	−37.807	6.6	1469	1200–1270	Humid

[a] Fick and Hijmans (2017).
[b] Owen et al. (2011).
[c] Muñoz et al. (2007).

from the three replicate volumetric samples per depth increment and not corrected by the amount of coarse fragments (> 2 mm). Texture analysis was performed after Blume et al. (2011) according to DIN ISO 11277. Seven fractions were determined with combined sieving of the fractions > 20 µm and pipette method of the fractions < 20 µm using 1000 mL Köhn cylinders.

Soil pH was determined with a 0.01 M $CaCl_2$ solution (soil-to-solution ratio 1:2.5) by a WTW pH meter pH 340 (WTW GmbH, Weilheim, Germany) using a Sentix 81 electrode according to DIN EN 15933.

The effective cation exchange capacity (CEC_{eff}) was determined for carbonate-free samples (all locations except for AZ) after Lüer and Böhmer (2000). A total of 2.5 g soil (< 2 mm) were dried at 40 °C and subsequently extracted with a 1 M NH_4Cl solution. The exchangeable cations (Ca^{2+}, Mg^{2+}, K^+, Na^+, Fe^{2+}, Mn^{2+}, Al^{3+}) were then measured by inductively coupled plasma - optical emission spectroscopy (ICP-OES, Optima 5300 DV, Perkin Elmer, USA) with a Miramist nebulizer and a cyclone chamber. The following wavelengths were used for the respective cations: Ca^{2+} (317.933 nm), Mg^{2+} (280.271 nm), K^+ (760.490 nm), Na^+ (589.592 nm), Fe^{2+} (283.204 nm), Mn^{2+} (257.61 nm), Al^{3+} (396.153 nm). Exchangeable protons (H^+) were determined as difference in the pH of the NH_4Cl solution before and after extraction. The effective BS was calculated as the percentage of the sum of exchangeable base cations (Ca^{2+}, Mg^{2+}, K^+, Na^+) from CEC_{eff}. For total C, N and S analyses, about 30 mg (two replicates) of finely milled sample material was weighed into tin foil and analyzed using oxidative heat combustion at 1150 °C in a helium atmosphere in a Vario EL elemental analyzer (Elementar Analysensysteme GmbH, Hanau, Germany).

The TOC content of samples with pH_{CaCl2} > 6.7 was corrected for the inorganic C from carbonates.

The carbonate content was determined volumetrically by CO_2, which evolved from the reaction with HCl, using a Calcimeter (Eijkelkamp, Giesbeek, Netherlands).

The measurement of stable carbon and nitrogen isotope ratios ($\delta^{13}C_{TOC}$, $\delta^{15}N$) was conducted using an isotope ratiomass spectrometer (Delta Plus with Confo III and a Flash Elemental Analyzer, Thermo Fisher Scientific, Bremen, Germany). As pretreatment, samples were dried (130 °C until constant weight) and milled. Samples from AZ were additionally decarbonized with 1 M HCl for 24 h to remove carbonates. The delta notation was calculated against the VPDB standard for carbon isotopes and air for nitrogen isotopes.

To determine plant-available phosphorus (P), 2 g of air-dried soil were extracted with 20 mL of Bray-1 extracting solution (0.025 M HCl + 0.03 M NH_4F, pH 2.6) according to Bray and Kurtz (1945). The inorganic phosphate concentrations in the extracts were determined photometrically by the molybdenum-blue method (Murphy and Riley, 1962) using a platereader (M200 pro, Tecan, Switzerland). To avoid the inhibiting effect of fluoride ions on the formation of the blue color complex, 0.1 M boric acid was used to bind the fluoride (Kurtz, 1942).

Pedogenic oxides of iron (Fe) and aluminum (Al), manganese (Mn) and silicon (Si) were determined with the dithionite-citrate method as described by Mehra and Jackson (1958). Active oxides of the same elements were examined as ammonium-oxalate extractable compounds (Schwertmann, 1964). Oxides associated with soil organic matter (SOM) were extracted with a 0.1 M pyrophosphate reagent ($Na_2P_2O_7$ 10 H_20). Elements have been analyzed with an inductively coupled plasma mass spectrometry (ICP-MS 7700× Agilent Technologies, Waldbronn, Germany).

2.4. Analysis of microbial abundance

Total genomic DNA was extracted using the PowerSoil® DNA Isolation Kit (MoBio Laboratories, CA, USA) for soil samples from LC, SG and NA (maximum amount of 0.25 g per sample). Samples from AZ were treated with the PowerMax® Soil DNA Isolation Kit (MoBio Laboratories, CA, USA) and were milled before processing (10 g of sample). Soil DNA was extracted in triplicates following the manufacturer's protocol with one exception: DNA elution was done with PCR-grade water. Final DNA concentrations were measured with a NanoPhotometer® (P360, Implen GmbH, München, Germany) and the purity was controlled by the value of optical density (OD_{260}/OD_{280} and OD_{260}/OD_{230}).

Gene copy numbers of bacteria and archaea were determined by quantitative polymerase chain reaction (qPCR). 16S rRNA genes were amplified by using the bacterial primer pair Eub341F (5′-CCT ACG GGA GGC AGC AG-3′) and Eub534R (5′-ATT ACC GCG GCT GCT GG-3′) (Muyzer et al., 1993) and the archaeal primer pair 340F (5′-CCC TAC GGG GYG CAS CAG-3′) and 1000R (5′-GGC CAT GCA CYW CYT CTC-3′) (Gantner et al., 2011). The qPCR assay was carried out in a total reaction volume of 20 µL using the KAPA SYBR® FAST qPCR Kit Master Mix (2×) Universal (Kapa Biosystems, Sigma-Aldrich, Germany) in accordance with the manufacturer's recommendations. Quantification was performed in the CFX96 Connect™ Real-Time System (Bio-Rad Laboratories, CA, USA) with the following cycling program for bacterial 16S rRNA genes (and for archaeal 16S rRNA genes in brackets): initial denaturation at 95 °C for 3 min, followed by 40 (45) cycles of denaturation at 95 °C for 3 s, annealing at 60 °C (57 °C) for 20 s, elongation at 72 °C for 30 s. Fluorescence was measured at 80 °C. The melting curve was recorded by rising temperature from 65 to 95 °C. Due to preliminary experiments, DNA extracts were used in 1:100 dilutions to avoid putative inhibitions of co-extracted substrates. Each sample was run in quadruplicates. Every qPCR run included blanks and calibration standards in triplicates. The reaction efficiency ranged between 98.8 and 102.0%. Data analysis was carried out using the CFX Manager™ Software (Bio-Rad Laboratories, CA, USA).

2.5. Vegetation and biocrusts characterization

The biocrust composition and cover on north- and south-facing slopes were characterized in 10 × 10 m plots, next to the mid-slope soil pits, during spring months in 2016. Percentage cover per species was estimated by measuring the cover of representative plants of each species and multiplying this by the number of individuals (the percentages were rounded to counting numbers). Leaf area index (LAI) measurements were obtained in a representative plot per site, using a Licor LAI-2200C Plant Canopy Analyzer, averaging nine measurements per plot.

Field surveys of dominant biocrust types were done at all four study areas in close proximity to the soil pits. The occurrence of biocrusts was visually estimated according to Williams et al. (2017), and lichens identified based on morphological traits. The observed biocrusts were sampled for the subsequent analysis of the community structure of the most abundant phototrophic microorganisms. For the taxonomic identification of cyanobacteria and microalgae, enrichment cultures and unialgal cultures were used in combination with direct microscopy. To obtain enrichment cultures, small amounts of material (c. 2 × 2 mm) were taken randomly out of the crust and placed on the surface of solid 1 N Bold's Basal Medium (1 N BBM), which were prepared with 1.5% agar in Petri dishes according to the methodological approach of Schulz et al. (2016). Phototrophs were morphologically identified by direct microscopy using an inverted light microscope (Olympus IX70) with 400-fold and/or 1000-fold magnification, depending on size of soil particles within the crust samples (Schulz et al., 2016).

2.6. Statistical analyses

Statistical analyses were conducted by using the software R (R Core Team, 2017). The R software packages car (Fox and Weisberg, 2011), GGplot (Wickham, 2009), Corrplot (Wei and Simko, 2017), Corrgram (Wright, 2017), Hmisc (Harrell and Dupont, 2017), and Rcmdr (Fox and Bouchet-Valat, 2017) were used. A factorial analysis of variance (ANOVA) was performed to evaluate the effects of climate, aspect and

topography of the physico-chemical and microbiological parameters within and between the study sites. Based on the study design, we performed the analysis on the depth increment datasets with one replicate of each slope position. Normality and variance homogeneity of the dataset were tested prior to ANOVA. Pair-wise differences were tested by using Tukey's HSD post hoc test. Unless otherwise stated p values ≤ 0.05 were considered as significant. Relations between parameters were evaluated by Pearson's correlation coefficient after testing for normality and log transformation.

3. Results

In the following sections, we present the results of the study sites structured according to our hypotheses addressing the climate gradient (regional scale) across all study sites, the catenas (local hillslope scale) and aspect in all study sites.

We analyzed the climate- and soil moisture-related trend for each soil property by using a local polynomial regression fitting (LOESS) (Cleveland et al., 1992). Based on this, we were able to address and visualize the regional climate gradient of the investigated soil properties (Fig. 4).

The sites are ranked from arid to humid site and differences between sites, e.g. the regional climate gradient is presented by the differing letters as a result of ANOVA. The profiles within the sites are ordered from the drier north-facing slope to moister south-facing upper slope, south-facing mid slope and the most moisture receiving south-facing lower slope showing the local variation within one study site.

3.1. Climate gradient

3.1.1. Vegetation and biocrusts

In the northern most arid site (AZ, Fig. 1), vegetation cover was < 5% with just single individuals of small desert shrubs, confined to moister microsites at some distance to the soil pits (*Tetragonia maritima*, *Nolana mollis*, *Perityle* sp. and *Stipa plumosa* on the south-facing slope; *Nolana mollis* and *Cristaria integerrima* on the north-facing slope, Table S5, Bernhard et al., 2018). From these species only *Tetragonia maritima*, *Nolana mollis* and *Cristaria integerrima* maintain their vegetative structures during dry periods, while the others appear annually. The water-restricted AZ was dominated by biocrusts (Table S6, Bernhard et al., 2018). The most arid site exhibited mainly desiccation tolerant chlorolichen-biocrusts throughout the year, with a comprehensive coverage of up to 40% of soil surface (Table S6, Bernhard et al., 2018). Dominant algal members were eukaryotic algae from the genera *Trebouxia* and *Elliptochloris*, which are common photobionts in chlorolichens. Detailed analysis of biocrust-forming phototrophic microorganisms showed that within the arid site biocrusts were formed almost exclusively by green algae, with cyanobacteria present only locally, i.e. mainly underneath quartz pebbles (Table S6, Bernhard et al., 2018).

In the semiarid climate of SG, the vegetation showed heights of about 1.5 m and a cover of 30–40%. It consisted of shrubs (*Proustia cuneifolia*, *Balbisia peduncularis* and *Senna cumingii* on the south-facing slope; *Cordia decandra*, *Adesmia* sp. and *Baccharis paniculatum* on the north-facing slope), many of which are drought-deciduous, and several types of cacti (*Eulychnia acida*, ≤2.5 m height and *Cumulopuntia sphaerica*, 0.04–0.25 m height). Even though higher plants are the dominant vegetation, biocrusts covered 10–15% of the soil surface of the inspected study area at SG. The transitional biocrust type, consisting of bryophytes, liverworts (*Riccia* spp.) and chlorolichens (*Placidium* sp., *Caloplaca* sp., *Acaraospora* spp.) dominated the SG cryptogamic vegetation cover during the dry season of the year (Table S6, Bernhard et al., 2018). Cyanobacteria were more abundant than eukaryotic algae in the community, and particularly the colonial N-fixing *Nostoc commune* is a major source of nitrogen in soils.

In the mediterranean climate of LC, vegetation had a cover of 100%. The south-facing slope was dominated by a canopy of evergreen-sclerophyllous forest of 3.5–9 m height (*Lithraea caustica* and *Colliguaja odorifera*), endemic tall palms (*Jubaea chilensis*), a tall deciduous shrub layer of 1–2.5 m height (*Podanthus mitiqui* and *Aristeguietia salvia* on the

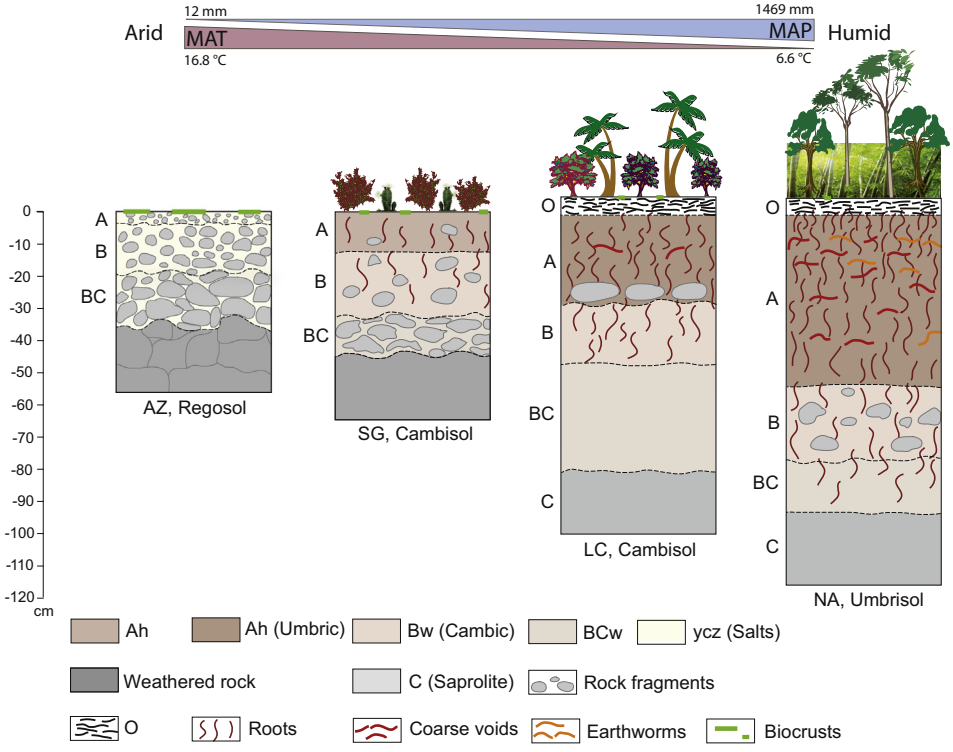

Fig. 2. Soil Reference Groups (after IUSS Working Group WRB, 2015) and mean soil depth and depth of A horizons of the south-facing slope profiles along the climate gradient for the primary study areas Pan de Azúcar (AZ), Santa Gracia (SG), La Campana (LC), Nahuelbuta (NA).

Table 2
Summary of mean soil physical, chemical and microbiological parameters (for original data cf. Table S2, Bernhard et al., 2018) for the north-facing mid slope (NMS), south-facing upper slope (SUS), south-facing mid slope (SMS) and south-facing lower slope (SLS) in all study sites Pan de Azúcar (AZ), Santa Gracia (SG), La Campana (LC) and Nahuelbuta (NA). Depth increment (DI) 1–4 (0–5, 5–10, 10–20, 20–40 cm, WM = depth related weighted mean, BD = bulk density, CEC_{eff} = cation exchange capacity, BS = base saturation, TOC = total organic carbon, Fe_{ox}/Fe_d = oxalate extractable iron/dithionite extractable iron, n.d. = not determined.

Site and position	Depth	Sand	Silt	Clay	Texture[a]	BD	pH	CEC_{eff}	BS	Plant-available P	TOC	C/N	$\delta^{13}C_{TOC}$	Fe_{ox}/Fe_d	DNA amount	Bacterial gene copy numbers	Archaeal gene copy numbers
DI	[cm]		[%]			[$Mg\,m^{-3}$]		[$\mu mol_c\,g^{-1}$]	[%]	[$mg\,kg^{-1}$]	[%]		[‰]		[$\mu g\,g^{-1}$]$_{soil}$	[g^{-1}]$_{soil}$	
AZ NMS																	
1	0–5	68	21	11	SaLo	1.2	8.0	n.d.	n.d.	0.4	< 0.09	n.d	−25.3	0.2	23.99 ± 15.3	2.30E+08 ± 2.33E+08	1.17E+06 ± 1.14E+06
2	5–10	79	12	9	SaLo	1.4	8.1	n.d.	n.d.	0.3	< 0.09	n.d	−24.1	0.1	14.99 ± 16.0	1.13E+06 ± 1.13E+06	3.32E+04 ± 1.20E+04
3	10–20	71	11	18	SaLo	1.3	8.1	n.d.	n.d.	1.6	< 0.09	n.d	−24.6	0.1	17.54 ± 18.4	2.92E+05 ± 1.64E+05	3.46E+04 ± 7.97E+03
4	20–40	54	28	19	SaLo	n.d.	8.0	n.d.	n.d.	5.5	< 0.09	n.d	−25.8	0.1	17.00 ± 16.7	3.64E+05 ± 2.44E+05	4.01E+04 ± 1.29E+04
WM		63	21	16	n.d.	1.3	8.0	n.d.	n.d.	3.2	< 0.09	n.d	−25.3	0.1	17.76 ± 17.0	2.91E+07 ± 1.53E+08	1.79E+05 ± 7.53E+05
AZ SUS																	
1	0–5	57	27	16	SaLo	1.3	8.1	n.d.	n.d.	0.1	0.1	4	−27.5	0.1	18.75 ± 4.4	3.72E+06 ± 3.61E+06	5.91E+04 ± 2.98E+04
2	5–10	56	28	16	SaLo	1.2	8.2	n.d.	n.d.	0.2	0.2	10.1	−23.3	0.1	22.75 ± 5.4	1.78E+05 ± 3.99E+04	2.33E+04 ± 1.22E+04
3	10–20	44	33	23	Lo	n.d.	8.2	n.d.	n.d.	0.2	0.2	13.8	−26.2	0.1	42.80 ± 26.0	1.04E+05 ± 4.01E+04	2.61E+04 ± 1.57E+04
4	20–40	41	46	13	Lo	n.d.	8.0	n.d.	n.d.	0.1	0.1	9.1	−28.3	0	33.30 ± 15.6	2.12E+05 ± 8.16E+04	2.73E+04 ± 2.46E+03
WM		46	38	16	n.d.	1.3	8.1	n.d.	n.d.	0.2	0.1	9.8	−27.1	0.1	32.50 ± 18.2	6.19E+05 ± 2.31E+06	3.05E+04 ± 2.28E+04
AZ SMS																	
1	0–5	62	26	12	n.d.	1.3	8.0	n.d.	n.d.	0.7	n.d.	n.d.	−26	n.d.	30.95 ± 11.6	2.43E+07 ± 2.33E+07	5.76E+05 ± 5.66E+05
2	5–10	76	15	10	LoSa	1.6	8.1	n.d.	n.d.	2.9	< 0.09	n.d.	−25.2	n.d.	22.41 ± 17.1	1.83E+05 ± 3.42E+04	2.44E+04 ± 3.60E+03
3	10–20	71	18	11	SaLo	n.d.	8.3	n.d.	n.d.	0.2	< 0.09	n.d.	−25.3	0	38.70 ± 24.8	5.69E+05 ± 1.97E+05	3.08E+04 ± 9.23E+03
4	20–40	n.d.	n.d.	n.d.	n.d.	n.d.	n.d.	n.d.	n.d.	n.d.	n.d.	n.d.	n.d.	n.d.	36.00 ± 12.6	1.65E+05 ± 2.27E+04	3.41E+04 ± 6.55E+03
WM		70	19	11	n.d.	1.5	8.2	n.d.	n.d.	1	< 0.09	n.d.	−25.5	0	34.35 ± 18.4	3.29E+06 ± 1.52E+07	9.98E+04 ± 3.60E+05
AZ SLS																	
1	0–5	68	23	10	SaLo	1.2	8.1	n.d.	n.d.	0.1	< 0.09	n.d.	−26.6	0.1	21.00 ± 1.9	3.80E+07 ± 3.07E+07	8.99E+05 ± 9.75E+05
2	5–10	67	21	12	SaLo	1.4	8.1	n.d.	n.d.	0.3	< 0.09	n.d.	−24.5	0.1	29.36 ± 29.5	2.23E+05 ± 7.78E+04	2.58E+04 ± 1.89E+04
3	10–20	44	44	12	Lo	n.d.	8.2	n.d.	n.d.	0.2	< 0.09	n.d.	−26.3	0	18.00 ± 18.4	6.34E+05 ± 5.02E+05	3.18E+04 ± 2.01E+04
4	20–40	n.d.	n.d.	n.d.	n.d.	n.d.	n.d.	n.d.	n.d.	n.d.	n.d.	n.d.	n.d.	n.d.	52.60 ± 12.3	2.12E+05 ± 5.11E+04	4.76E+04 ± 2.34E+04
WM		56	33	11	n.d.	1.3	8.2	n.d.	n.d.	0.2	< 0.09	n.d.	−25.9	0.1	37.10 ± 22.9	5.04E+06 ± 2.24E+07	1.47E+05 ± 6.15E+05
SG NMS																	
1	0–5	72	16	12	SaLo	1.5	6.2	81	99	62.6	0.4	10.2	−22.4	0.6	57.10 ± 2.2	5.84E+08 ± 4.43E+07	3.89E+07 ± 4.75E+06
2	5–10	76	13	11	SaLo	1.5	6.2	82	99	42.8	0.4	11.2	−21.6	0.3	32.00 ± 1.9	1.31E+08 ± 3.73E+07	8.82E+06 ± 2.49E+06
3	10–20	67	14	19	n.d.	1.5	5.8	153	100	88.5	n.d.	n.d.	−21.7	n.d.	29.00 ± 1.4	5.95E+07 ± 2.13E+07	4.70E+06 ± 1.82E+06
4	20–40	62	13	25	SaClLo	1.7	6.0	176	100	9.8	0.3	9.5	−22.3	0.4	22.75 ± 2.4	2.17E+07 ± 6.57E+06	1.18E+06 ± 6.44E+05
WM		66	14	20	n.d.	1.6	6.0	146	100	40.2	0.3	9.9	−22.1	0.4	29.76 ± 13.2	1.15E+08 ± 2.25E+08	7.73E+06 ± 1.51E+07
SG SUS																	
1	0–5	77	16	8	SaLo	1.6	6.9	81	99	46.3	0.7	11.6	−25	0.6	48.60 ± 8.8	4.10E+08 ± 1.68E+08	2.41E+07 ± 1.24E+07
2	5–10	77	16	8	SaLo	1.5	6.6	62	100	36.6	0.5	10.6	−24.2	0.5	45.50 ± 6.1	2.50E+08 ± 5.06E+07	2.11E+07 ± 4.23E+06
3	10–20	75	16	10	SaLo	1.5	6.6	85	100	39.7	0.5	10.6	−23.3	0.4	39.75 ± 5.3	1.63E+08 ± 1.33E+07	1.49E+07 ± 3.21E+05
4	20–40	76	14	10	SaLo	1.6	6.8	87	100	30	0.3	9.7	−23.1	0.6	26.50 ± 2.2	4.39E+07 ± 2.16E+07	2.91E+06 ± 1.44E+06
WM		76	15	9	n.d.	1.5	6.7	83	100	35.3	0.4	10.3	−23.5	0.5	34.95 ± 10.4	1.45E+08 ± 1.60E+08	1.08E+07 ± 1.05E+07
SG SMS																	
1	0–5	77	16	7	LoSa	1.5	6.3	50	98	33.1	0.7	12.2	−26.1	1.1	55.85 ± 12.7	4.02E+08 ± 2.68E+08	2.15E+07 ± 1.47E+07
2	5–10	77	16	7	LoSa	1.5	6.4	59	100	19.2	0.5	13.2	−25.3	0.8	45.40 ± 4.3	2.71E+08 ± 3.45E+07	2.15E+07 ± 7.74E+06
3	10–20	80	13	7	LoSa	1.5	6.4	68	100	7.9	0.5	13.8	−24.2	0.7	39.75 ± 2.5	1.67E+08 ± 2.06E+07	1.26E+07 ± 2.05E+06
4	20–40	78	14	8	SaLo	1.5	6.2	68	100	6.3	0.3	11.7	−24	0.8	30.25 ± 1.1	6.64E+07 ± 1.29E+07	4.09E+06 ± 7.96E+05
WM		78	14	8	n.d.	1.5	6.3	65	100	11.7	0.4	12.5	−24.5	0.8	37.72 ± 11.5	1.59E+08 ± 1.84E+08	1.06E+07 ± 1.11E+07
SG SLS																	
1	0–5	77	17	7	LoSa	1.6	6.3	67	99	34.6	0.6	10.1	−25.7	0.4	58.40 ± 5.0	5,55E+08 ± 5.15E+07	3.78E+07 ± 1.26E+07
2	5–10	78	15	7	LoSa	1.5	6.4	66	100	57.5	0.3	9.7	−25.1	0.2	41.00 ± 4.1	1,99E+08 ± 3.35E+07	2.11E+07 ± 5.32E+06
3	10–20	75	17	8	SaLo	1.5	6.6	61	100	51.9	0.4	10.6	−24.5	0.9	34.75 ± 1.5	1,01E+08 ± 1.59E+07	1.11E+07 ± 3.72E+06
4	20–40	78	15	8	LoSa	1.5	6.3	64	100	41	0.4	10.7	−23.7	0.7	35.05 ± 6.7	1,16E+08 ± 4.50E+07	6.93E+06 ± 3.36E+06
WM		77	15	8	n.d.	1.5	6.4	64	100	45	0.4	10.5	−24.3	0.6	38.64 ± 10.71	1.78E+08 ± 1.94E+08	1.36E+07 ± 1.46E+07
LC NMS																	
1	0–5	71	20	10	SaLo	1.3	6.0	162	99	17.2	3.1	15.2	−26.4	0.4	83.80 ± 6.4	5.98E+08 ± 6.68E+07	2.47E+07 ± 7.55E+06

(*continued on next page*)

Table 2 (*continued*)

Site and position	Depth	Sand	Silt	Clay	Texture[a]	BD	pH	CEC_{eff}	BS	Plant-available P	TOC	C/N	$\delta^{13}C_{TOC}$	Fe_{ox}/Fe_d	DNA amount	Bacterial gene copy numbers	Archaeal gene copy numbers
DI	[cm]		[%]			[$Mg\,m^{-3}$]		[$\mu mol_c\,g^{-1}$]	[%]	[$mg\,kg^{-1}$]	[%]		[‰]		[$\mu g\,g^{-1}$]$_{soil}$	[g^{-1}]$_{soil}$	
2	5–10	71	21	8	SaLo	1.4	5.6	84	99	33.5	1.7	15.9	−25.9	0.2	37.45 ± 5.6	1.31E+08 ± 6.24E+07	4.71E+06 ± 1.78E+06
3	10–20	73	18	9	SaLo	1.5	5.4	69	99	44.4	0.7	14.8	−24.9	0.3	35.00 ± 5.4	9.18E+07 ± 2.25E+07	3.92E+06 ± 8.04E+05
4	20–40	69	19	13	SaLo	1.5	5.0	70	99	14.8	0.6	14.6	−24.1	0.2	30.50 ± 3.0	6.07E+07 ± 1.52E+07	1.08E+07 ± 6.65E+06
WM		70	19	11	n.d.	1.5	5.3	83	99	24.8	1.1	14.9	−24.8	0.2	39.16 ± 22.2	1.44E+08 ± 2.25E+08	1.01E+07 ± 9.76E+06
LC SUS																	
1	0–5	72	19	9	SaLo	1.3	5.5	210	99	5.6	4.6	17.2	−26.3	0.3	67.90 ± 7.1	3.58E+08 ± 9.69E+07	1.03E+07 ± 2.13E+06
2	5–10	72	19	8	SaLo	1.3	5.4	97	99	3.7	1.8	14.7	−26.2	0.3	37.05 ± 9.8	1.96E+08 ± 9.72E+07	4.55E+06 ± 2.31E+06
3	10–20	72	20	8	SaLo	1.4	5.3	64	99	9.5	1.1	13.8	−26.1	0.3	34.75 ± 0.8	1.57E+08 ± 2.53E+07	5.16E+06 ± 1.91E+06
4	20–40	74	18	9	SaLo	1.5	5.0	54	99	9.3	0.7	13.4	−25.6	0.3	31.50 ± 5.0	1.09E+08 ± 3.70E+07	1.37E+07 ± 8.12E+06
WM		73	19	9	n.d.	1.4	5.2	81	99	8.2	1.4	14.1	−25.9	0.3	37.56 ± 16.0	1.63E+08 ± 1.18E+08	1.00E+07 ± 5.84E+06
LC SMS																	
1	0–5	72	18	10	SaLo	0.8	5.8	318	99	7.9	7.8	17.1	−26.7	0.5	102.60 ± 31.9	6.86E+08 ± 2.87E+08	5.73E+07 ± 5.75E+07
2	5–10	73	16	11	SaLo	1	5.7	190	100	6.8	4.8	15.1	−26.4	0.4	74.30 ± 8.1	4.69E+08 ± 1.38E+08	2.08E+07 ± 1.72E+07
3	10–20	74	15	11	SaLo	1.2	5.5	134	100	4.6	2.2	13.8	−25.9	0.4	67.90 ± 17.8	3.34E+08 ± 1.36E+08	2.00E+07 ± 1.33E+07
4	20–40	75	15	10	SaLo	1.2	5.3	87	100	4.6	1.3	13.6	−25.5	0.4	45.35 ± 6.9	2.17E+08 ± 7.56E+07	1.70E+07 ± 7.06E+06
WM		74	15	10	n.d.	1.1	5.4	141	100	5.3	2.8	14.3	−25.9	0.4	61.76 ± 27.9	3.36E+08 ± 2.73E+08	2.33E+07 ± 3.92E+07
LC SLS																	
1	0–5	69	18	13	SaLo	1.2	5.9	223	99	56	6.4	21.8	−26.5	0.4	59.80 ± 13.0	4.40E+08 ± 1.87E+08	2.01E+07 ± 9.82E+06
2	5–10	69	18	13	SaLo	1.3	5.9	191	100	28.7	3.4	16.4	−26	0.3	61.30 ± 5.6	2.47E+08 ± 1.09E+08	1.55E+07 ± 6.73E+06
3	10–20	70	18	12	SaLo	1.3	5.8	123	100	20.9	1.8	14.3	−25.8	0.3	53.20 ± 9.3	2.11E+08 ± 9.76E+07	2.02E+07 ± 1.17E+07
4	20–40	73	15	12	SaLo	1.2	5.9	105	100	8.6	1	14.1	−25.7	0.3	40.25 ± 12.6	1.78E+08 ± 5.62E+07	1.67E+07 ± 8.88E+06
WM		71	17	12	n.d.	1.2	5.9	135	100	20.1	2.2	15.4	−25.9	0.3	48.56 ± 13.43	2.28E+08 ± 1.59E+08	1.79E+07 ± 9.67E+06
NA NMS																	
1	0–5	51	25	24	SaClLo	0.8	4.5	52	43	2.7	6.3	21	−25.2	0.9	60.80 ± 17.8	3.05E+08 ± 1.15E+08	5.27E+06 ± 2.25E+06
2	5–10	56	23	21	SaClLo	0.8	4.5	45	28	1.7	5.5	21.6	−24.7	0.9	71.80 ± 15.0	2.57E+08 ± 3.06E+07	7.91E+06 ± 2.33E+06
3	10–20	50	26	23	SaClLo	0.9	4.4	45	24	1.3	6	20.3	−24.3	0.9	47.20 ± 25.8	1.87E+08 ± 1.47E+08	7.65E+06 ± 7.04E+06
4	20–40	50	25	25	SaClLo	1	4.6	31	20	1	4.5	19.3	−24.8	1	22.50 ± 3.9	7.30E+07 ± 3.06E+07	1.42E+07 ± 1.36E+07
WM		51	25	24	n.d.	0.9	4.5	39	25	1.4	5.2	20.1	−24.7	0.9	39.63 ± 25.4	1.54E+08 ± 1.30E+08	1.07E+07 ± 8.49E+06
NA SUS																	
1	0–5	55	22	23	SaClLo	0.6	3.6	124	13	1.6	12.6	26.8	−25.8	1.4	73.60 ± 6.8	1.20E+08 ± 5.26E+07	2.02E+06 ± 4.50E+05
2	5–10	56	20	24	SaClLo	0.7	4.0	74	9	0.9	7.5	24.6	−25.6	1.3	91.80 ± 17.9	2.19E+08 ± 7.26E+07	4.26E+06 ± 1.65E+06
3	10–20	55	22	23	SaClLo	0.8	4.2	64	8	0.8	6.4	23.6	−25.6	1.3	57.10 ± 3.8	2.48E+08 ± 3.31E+07	6.18E+06 ± 1.01E+06
4	20–40	54	22	25	SaClLo	0.9	4.4	47	8	0.3	4	22.6	−25.4	1.2	67.80 ± 8.3	2.80E+08 ± 5.35E+07	1.15E+07 ± 2.98E+06
WM		55	22	24	n.d.	0.8	4.2	64	9	0.7	6.1	23.6	−25.5	1.3	68.85 ± 16.5	2.44E+08 ± 8.12E+07	8.08E+06 ± 3.93E+06
NA SMS																	
1	0–5	52	22	26	SaClLo	0.7	4.1	85	27	1.9	8.6	21.1	−25.3	0.9	75.60 ± 21.2	2.35E+08 ± 9.76E+07	5.27E+06 ± 3.01E+06
2	5–10	52	22	27	SaClLo	0.7	4.2	70	13	1.8	7.3	21.1	−24.8	1.1	92.50 ± 15.0	3.14E+08 ± 5.57E+07	7.67E+06 ± 2.56E+06
3	10–20	50	23	28	SaClLo	0.8	4.2	58	11	1.9	6.3	21.2	−24.6	0.4	80.60 ± 31.6	3.11E+08 ± 6.49E+07	9.56E+06 ± 1.15E+06
4	20–40	48	22	30	SaClLo	0.8	4.4	41	8	1.5	4.5	21	−24.3	0.8	64.00 ± 20.7	2.59E+08 ± 3.64E+07	1.99E+07 ± 2.61E+07
WM		49	22	29	n.d.	0.7	4.3	54	12	1.7	5.8	21.1	−24.6	0.8	73.16 ± 25.1	2.76E+08 ± 7.40E+07	1.40E+07 ± 1.58E+07
NA SLS																	
1	0–5	47	24	29	SaClLo	0.6	4.5	87	62	1.5	9.7	19	−25.1	1.5	100.20 ± 9.2	4.83E+08 ± 2.12E+08	8.18E+06 ± 2.53E+06
2	5–10	47	24	29	SaClLo	0.6	4.2	67	34	1.8	9	20.4	−24.6	1.2	102.10 ± 14.8	2.14E+08 ± 3.26E+07	3.98E+06 ± 2.29E+06
3	10–20	46	25	30	SaClLo	0.8	4.3	63	29	1.1	8.4	19.9	−24.4	1.2	57.40 ± 16.0	1.44E+08 ± 1.13E+08	7.57E+06 ± 1.19E+07
4	20–40	46	27	27	SaClLo	0.8	4.4	37	10	1	5.8	20.2	−24.6	1.5	53.60 ± 22.4	1.24E+08 ± 8.89E+07	3.87E+06 ± 2.80E+06
WM		46	26	28	n.d.	0.8	4.4	54	24	1.2	7.3	20	−24.6	1.4	66.44 ± 28.1	1.85E+08 ± 1.88E+08	5.35E+06 ± 7.00E+06

[a] Food and Agriculture Organization of the United Nations (FAO) (2006).

south-facing slope), and a highly abundant and diverse herb layer, rich in annual species (*Alstroemeria* sp., *Geranium robertianum*, *Stellaria media*, and the fern *Adiantum chilense*). On the north-facing slope, the tree canopy (*Lithraea caustica*, few *Jubaea chilensis*) and shrub layer (*Retamilla trinervia*, *Aristeguietia salvia*, *Colliguaja odorifera*) was more open and less rich in species. In the herbaceous layer (*Poaceae* spp. and *Sonchus oleraceus*), also climbing species (*Tropaeolum* sp., *Dioscorea* sp.) were found. The southernmost humid site NA had a vegetation cover of 100% with mixed forest, consisting of evergreen and winter-deciduous broadleaved trees in the canopy of about 14 m height on average (*Araucaria araucana* and *Nothofagus antarctica* on the south-facing slope; *Nothofagus obliqua* on the north-facing slope), with less density on the north-facing slope. The understory consisted of bamboo (*Chusquea coleu*) on the south-facing slope and *Gaultheria mucronata* on the north-facing slope, where also herbs (*Stipa* sp. and *Mutisia decurrens*) were very abundant. Similar to the increase of vegetation cover, LAI increased from close to zero (< 0.01) in the driest site AZ to 0.3 in SG to 2.8 in LC and 2.8 in the most humid site NA. In the mediterranean (LC) and humid (NA) sites, biocrusts covered only 1–5% of the soil surface. They occurred rather locally, mainly in heavily disturbed habitats, either natural or anthropogenic, where higher plants were removed or unable to grow. These biocrusts were composed of drought sensitive bryophytes, accompanied by the green algae *Klebsorimdium* sp., *Chlorococcum* sp., *Chlamydomonas* sp. and nitrogen-fixing cyanobacteria of the genus *Nostoc* (Table S6, Bernhard et al., 2018). However, it has to be mentioned that LC and NA were far less surveyed and sampled compared to the sites AZ and SG, hence, the relevance and abundance of biocrusts might be underestimated.

3.1.2. Pedogenesis

The soils showed distinct differences between the study sites along the climate gradient for almost all soil properties (Fig. 2, Table 2, Fig. 4).

Mainly Regosols, Cambisols and Umbrisols were classified (according to IUSS Working Group WRB, 2015) within the arid (AZ) to humid (NA) study sites (for field description see Table S1, Bernhard et al., 2018). The Regosols in AZ were marked by the occurrence of a thin A horizon with very low in the field detectable soil organic matter contents (< 0.4%) and a single grain structure under a thin pavement of coarse material (fine to medium gravel). The following B horizon contained pedogenic gypsum and large amounts of coarse material (> 2 mm). The Cambisols in SG had an Ah horizon with low soil organic matter contents (0.5–1.2%) and a subangular blocky structure. Only on the north-facing mid slope in SG, a shallower soil developed, e.g. a Leptosol. The Cambisols in LC had a soil organic matter content enriched Ah horizon (4–9%) with a granular structure. Within the lower slope profile in LC, the upslope occurring cambic (Bw) horizon was missing (Table S1, Bernhard et al., 2018), most likely due to erosion.

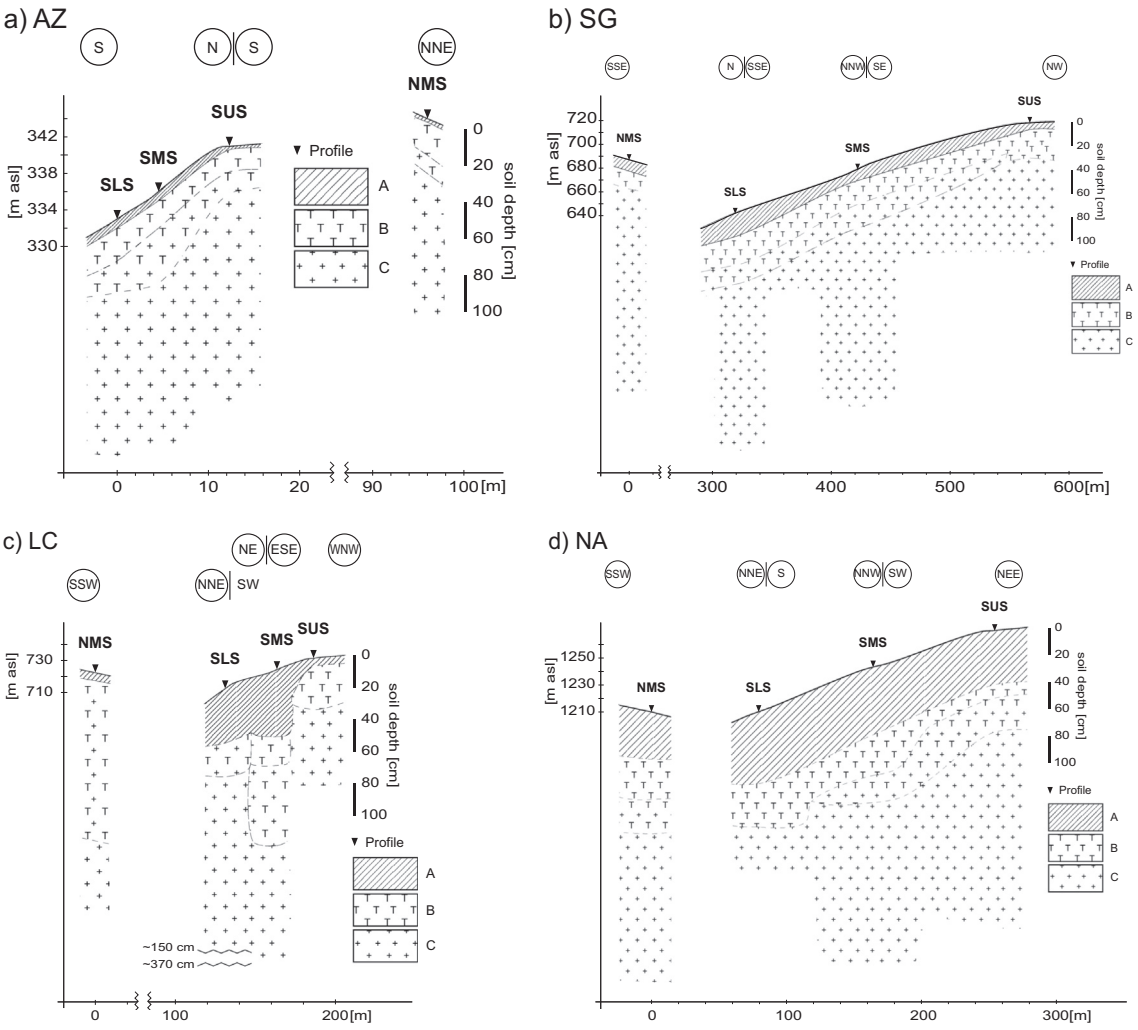

Fig. 3. a–d. Soil catenas along the south-facing slope with south-facing upper slope (SUS), south-facing mid slope (SMS), south-facing lower slope (SLS) and the additional profile on the north-facing slope (NMS): a) Pan de Azúcar (AZ), b) Santa Gracia (SG), c) La Campana (LC) and d) Nahuelbuta (NA). Note, the horizon depths were graphically interpolated between soil horizons.

This can be attributed to the much higher slope (35°) of the lower slope position compared to the mid slope (23°). Also a layer of weathered rock fragments of about 20 cm thickness occurred at the border of Ah to BCw horizon, indicating that the lower slope profile might have received material from upslope in a discrete event after being eroded. Also the midslope position might have received material from upslope as evidenced by weathered rock fragments sized 5–10 cm, that were found mostly aligned horizontally to the slope between Ah2 horizon and Ah3 horizon. In NA, Umbrisols were present with a dark colored, well-structured umbric horizon with a BS < 50%, a well-developed pedality and low BD, followed by a cambic horizon. The thick (35–53 cm) umbric Ah horizons had high soil organic matter contents with 9–15%. At the north-facing slope of NA, a Podzol was classified after WRB as having a spodic horizon from 65 to 90 cm depth (Table S1, Bernhard et al., 2018).

The stage of soil development differed between study sites with strong developed mineral subsoils in the southern mediterranean and humid study sites LC and NA (Fig. 2). The soil depth did not differ much between the arid (AZ) and semiarid (SG) region, but larger amounts of coarse material > 2 mm were found in the profiles of AZ (Table S1, Bernhard et al., 2018). Additionally, the thickness of the A horizon increased along the climate gradient from arid to humid climate (Fig. 3). In the arid and semiarid study sites, the C horizon consisted of weathered rock according to IUSS Working Group WRB (2015). In the mediterranean and humid study sites, saprolite was found. Taking into account the geochemical analyses of element depletion, the C horizons in all study areas can be classified as saprolite (Oeser et al., 2018).

Loamy sand and sandy loam textural classes were mainly present in the northern sites AZ and SG. The mediterranean site LC had mainly sandy loam textural class and the humid site NA had sandy-clay loam textural class (Table S1, Bernhard et al., 2018). In general, the average clay content increased from the semiarid site SG (12.0%) to the humid site NA (26.1%, Table 3), thus, the texture became finer with increasing humidity.

The most arid site AZ turned out to be an exception from this trend, especially with its higher silt and clay content in comparison to SG. Furthermore, the variability of sand and silt contents was higher than for SG, LC and NA (Table 3). The clay contents were significantly different between AZ-SG and LC-NA, but similar in SG and LC (Fig. 4c). The texture changed little with depth for 0–40 cm depth in all sites. The BD covered a very wide range from 1.7 Mg m^{-3} (SG) to 0.6 Mg m^{-3} (NA, Table 3) along the regional gradient for 0–40 cm depth. On average, the BD decreased significantly from semiarid (SG, 1.5 Mg m^{-3}) to mediterranean (LC, 1.3 Mg m^{-3}) to humid study site (NA, 0.8 Mg m^{-3}, Table 3, Fig. 4d). The BD of AZ (1.3 Mg m^{-3}) with its lower values compared to the semiarid site SG is an exception to this climate trend. The decrease of BD had a strong correlation to the increasing clay contents (r = −0.86***) and the increasing TOC (r = −0.91***, Table 4).

The BD decreased by about 31% within the C horizons from the mediterranean (1.6 Mg m^{-3}) to the humid study site (1.1 Mg m^{-3}, Table S3, Bernhard et al., 2018), hence, the saprolite had a higher porosity in humid climate. The BD increased within 0–40 cm depth in the mediterranean (LC) and humid (NA) study sites, only (Table 2). The activity ratio (Fe_{ox}/Fe_d ratio) increased on average from AZ (0.1) to LC (0.3) and from LC to NA (1.1, Table 3), but only LC and NA were significantly different (Fig. 4m). SG (0.6, Table 3) turned out to be an exception from the gradient with higher values compared to AZ and LC, but lower values in comparison with NA.

In summary, pedogenic processes such as soil depth, clay contents, porosity and activity ratio increased with increasing humidity.

3.1.3. Nutrient availability (pH value, CEC_{eff}, plant-available P, C/N, TOC) and isotope composition ($\delta^{13}C_{TOC}$)

The pH values varied from alkaline in AZ (pH 8.3) to very strong acidic in NA (pH 3.6). A significant decrease of values was observed from the northern arid (AZ, pH 8.2) to the semiarid (SG, pH 6.3), the mediterranean (LC, pH 5.4) and the southern humid study site (NA, pH 4.3, Table 3). The pH values changed little with depth in arid and semiarid climate, whereas they decreased in the mediterranean climate of LC and increased in the humid climate of NA with soil depth. In general, pH values and BS were strongly correlated (r = 0.85***). The BS ranged from 98.3 to 99.9% in SG and LC (Table 2), where mainly Ca^{2+} (71.3% and 84.4%, respectively) and Mg^{2+} (21.7% and 11.1%, respectively, Fig. 5) cations were present. In contrast, the average BS was significantly lower in NA (17.4%, Table 3) with a dominance of Al^{3+} cations (Fig. 5). Clay contents and BS were strongly negatively correlated (r = −0.92***, Table 4). The plant-available P ranged from 0.1 to 88.5 mg kg^{-1} in the whole study area (Table 2). The average was lowest in AZ and NA (1.2 mg kg^{-1}) and highest in SG (20.9 mg kg^{-1}). The values decreased along the regional gradient from SG to LC (14.6 mg kg^{-1}, Table 3) and to NA. Plant-available P was strongly positively correlated with the pH value (r = 0.85***, Table 4).

The TOC varied between < 0.09–12.6% and increased from arid to humid study site. The average values increased from close to zero (< 0.09%) in the northern arid site (AZ) to 0.4% in the semiarid site (SG) to 1.9% in the mediterranean site (LC) and 6.1% in the most humid site (NA, Table 3). The difference was significant between SG-LC and LC-NA, but not between AZ and SG (Fig. 4j). Characteristic for the TOC was the substantial decrease with depth in SG, LC and NA. Except for similar values in AZ and SG, the C/N ratio differed significantly between all other study sites and increased on average from the arid (AZ, 9.8) to humid (NA, 21.2, Table 3) study site. Average $\delta^{13}C_{TOC}$ values ranged for depth increments 1–4 between −21.5‰ and −29.2‰. They increased significantly from AZ (−25.9‰) to SG (−23.6‰) and decreased significantly from SG to LC (−25.6‰). An increasing trend was detected from LC to NA (−24.9‰, Table 3, Fig. 4l).

In summary, the results related to the climate gradient showed with

Table 3
Mean values of soil physical, chemical and microbiological parameters in all study sites Pan de Azúcar (AZ), Santa Gracia (SG), La Campana (LC) and Nahuelbuta (NA). SD = standard deviation, BD = bulk density, CEC_{eff} = cation exchange capacity, BS = base saturation, TOC = total organic carbon, Fe_{ox}/Fe_d = oxalate extracted iron/dithionite extracted iron, n.d. = not determined.

Site	Sand	Silt	Clay	BD	pH	CEC_{eff}	BS	Plant-available P	TOC	C/N	$\delta^{13}C_{TOC}$	Fe_{ox}/Fe_d	DNA amount	Bacterial gene copy numbers	Archaeal gene copy numbers
		[%]		[Mg m^{-3}]		[μmol$_c$ g^{-1}]	[%]	[mg kg^{-1}]	[%]		[‰]		[μg g^{-1}]$_{soil}$	[g^{-1}]$_{soil}$	
AZ Mean	58.6	27.6	13.8	1.3	8.1	n.d.	n.d.	1.2	< 0.09	9.8	−25.9	0.1	27.51	1.87E + 07	1.95E + 05
AZ SD	11.7	10.1	3.9	0.1	0.1	n.d.	n.d.	1.5	n.d.	n.d.	1.3	0.0	20	7.98E + 07	5.24E + 05
SD Mean	74.4	14.6	11.1	1.5	6.3	89.4	99.7	33.0	0.4	10.8	−23.6	0.6	40.1	2.21E + 08	1.58E + 07
SG SD	4.4	1.3	4.9	0.0	0.3	33.0	0.5	20.9	0.1	1.2	1.3	0.2	11.9	1.95E + 08	1.33E + 07
LC Mean	72.1	17.3	10.5	1.3	5.4	109.8	99.3	14.6	1.9	14.7	−25.6	0.3	53.92	2.80E + 08	1.66E + 07
LC SD	1.8	1.7	1.6	0.2	0.3	71.3	0.3	15.2	2.1	2.0	0.6	0.1	23.6	2.28E + 08	2.34E + 07
NA Mean	50.2	23.6	26.2	0.8	4.3	52.7	17.4	1.2	6.1	21.2	−24.9	1.1	69.91	2.36E + 08	5.16E + 06
NA SD	3.3	1.9	2.6	0.1	0.2	22.6	14.8	0.5	2.2	2.0	0.5	0.3	26.7	1.30E + 08	1.02E + 07

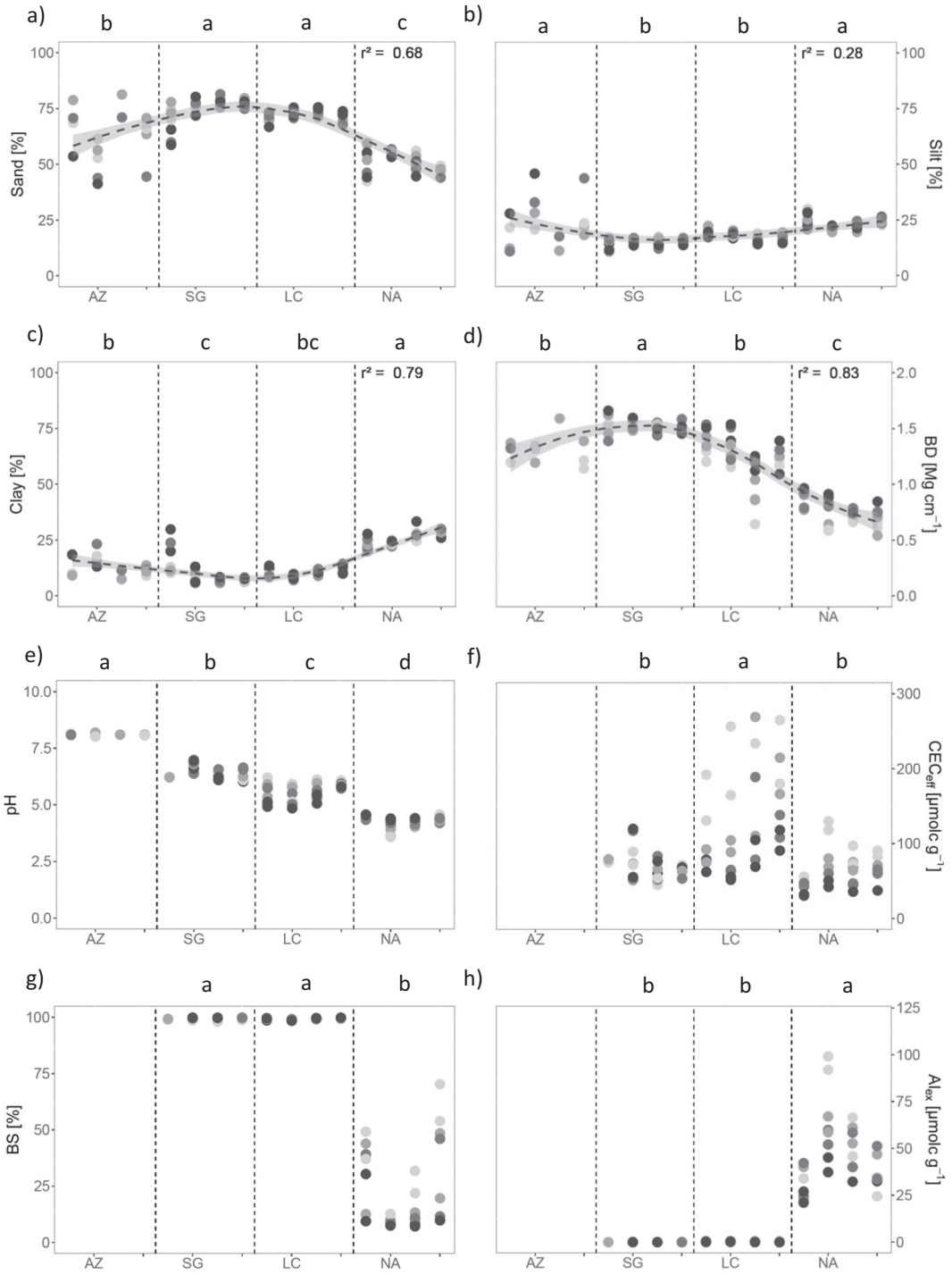

Fig. 4. a–p. ANOVA results for the regional transect.
Differing letters (a–d) indicate a significant difference of the mean values for DIs 1–4 in AZ, SG, LC, NA with $p < 0.05$. The order of topographic positions within each site is as follows: north-facing mid slope, south-facing upper slope, south-facing mid slope, south-facing lower slope. The fitted trend line has a confidence interval of 95% (grey area) and r^2 (rsq) shows the fit between values and trend line. For pH, CEC_{eff}, BS and Al_{ex} the trend line could not be fitted.

increasing humidity an increase of TOC, C/N and a decrease of pH value and plant-available phosphorus. Base saturation and Al_{ex} had a threshold-like distribution with significantly lower BS and higher Al_{ex} in the humid site (NA) compared to the semiarid and mediterranean sites (SG, LC). A general trend along the climate gradient was not observed for $\delta\ ^{13}C_{TOC}$.

3.1.4. Microbial abundances

The extraction of total genomic DNA revealed an increasing trend from the northern arid (AZ) to southern humid site (NA, Fig. 4n). Soil samples from AZ contained the lowest DNA amounts with a minimum of 0.4 µg g^{-1} soil (Table S4, Bernhard et al., 2018). DNA concentrations in SG varied between 20.5 ± 0.5 to 67.6 ± 4.4 µg g^{-1} soil. In contrast, the highest DNA amounts were detected in LC (134.6 ± 5.0 µg g^{-1} soil), especially with emphasis on the first two depth increments, and NA with a maximum of 107.6 ± 11.6 µg g^{-1} soil. Along the depth profiles, DNA concentrations in AZ revealed an increasing trend from 0 to 40 cm. In comparison, DNA amounts

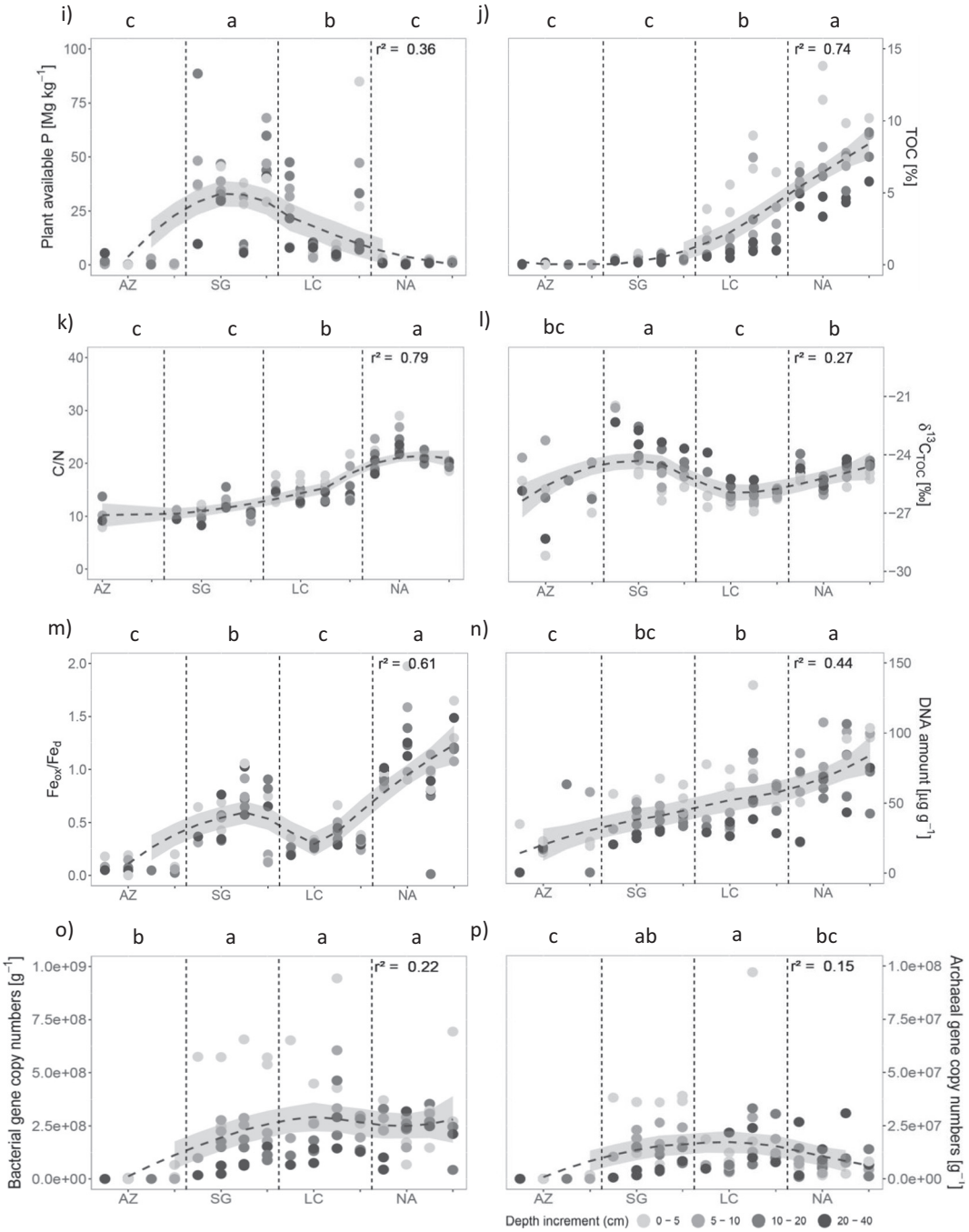

Fig. 4. (*continued*)

decreased with depth in SG and LC. Soil samples from NA revealed increasing DNA concentrations within the uppermost 10 cm, followed by a decrease down to 40 cm.

The quantification of 16S rRNA genes (Fig. 6), which are indicative for cell numbers, showed consistently higher abundances of bacteria than archaea in all soil samples (Table S4, Bernhard et al., 2018).

Despite the large climate variation of the study sites, only minor variations were found. Overall, AZ revealed a unique pattern in comparison to all other study sites. Here, bacterial and archaeal abundances were significantly lower and varied, except for the first depth increment for each slope, from 8.5×10^3 ($\pm 1.7 \times 10^3$) to 1.6×10^6 ($\pm 1.5 \times 10^6$) gene copies g^{-1} soil. In SG, LC and NA, bacterial abundances ranged from 10^8 to 10^9 gene copies g^{-1} soil (Fig. 6a–d), whereas archaeal numbers varied between 10^6 and 10^8 gene copies g^{-1} soil (Fig. 6e–h). The dataset, obtained from SG, LC and NA, is significantly different in comparison to the arid site AZ. Along the depth profiles, AZ revealed an initial drop of cell numbers by up to three orders of magnitude within the uppermost 5 cm and remained constant down to 40 cm. Similar to the DNA amounts, bacterial and archaeal abundances decreased with depth in SG and LC. The depth profiles of NA revealed higher variations (see Sections 3.2. and 3.3).

3.2. Catenas (local hillslope scale)

Along the catenas (Fig. 3a–d), the soil depth increased from the upper slope to lower slope in AZ and SG, whereas in LC and NA soil depth was greater at the mid slope. In all study sites, the soil on the north-facing mid slope was shallower than at the south-facing mid slope.

With regard to the ANOVA results for grain sizes, no significant

Table 4
Correlation matrix with correlation coefficients and significance (***: $p < 0.01$, **: $p < 0.05$; *: $p < 0.01$) for soil physical, chemical and microbiological parameters. Red colors indicate negative, blue colors positive correlation. BD = Bulk density, CEC_{eff} = cation exchange capacity, BS = base saturation, Plant a. P = Plant-available P, TOC = total organic carbon, Fe_{ox}/Fe_d = oxalate extracted iron/dithionite extracted iron, bacteria = bacterial gene copy numbers, archaea = archaeal gene copy numbers (cf. Table S2, Bernhard et al., 2018– for original data).

	Depth	Sand	Silt	Clay	BD	pH	CEC_{eff}	BS	Al_{ex}	Plant a. P	TOC	C/N	Fe_{ox}/Fe_d	DNA amount	Bacteria	Archaea
Depth		-0.02	-0.07	0.07	0.11	-0.07	-0.40 ***	-0.09	-0.09	-0.19	-0.26 *	-0.10	-0.03	-0.43 ***	-0.53 ***	-0.19
Sand			-0.92 ***	-0.98 ***	0.86 ***	0.86 ***	0.30 *	0.91 ***	-0.81 ***	0.81 ***	-0.81 ***	-0.82 ***	-0.58 ***	-0.43 ***	0.00	0.34 **
Silt		***		0.83 ***	-0.75 ***	-0.77 ***	-0.28 *	-0.78 ***	0.66 ***	-0.71 ***	0.76 ***	0.76 ***	0.44 ***	0.33 **	0.01	-0.33 **
Clay		***	***		-0.86 ***	-0.86 ***	-0.30 *	-0.92 ***	0.83 ***	-0.81 ***	0.78 ***	0.81 ***	0.60 ***	0.46 ***	-0.01	-0.33 **
BD		***	***	***		0.84 ***	0.00	0.82 ***	-0.81 ***	0.83 ***	-0.91 ***	-0.87 ***	-0.53 ***	-0.61 ***	-0.15	0.27 *
pH		***	***	***	***		0.24 *	0.85 ***	-0.83 ***	0.85 ***	-0.80 ***	-0.86 ***	-0.45 ***	-0.42 ***	0.06	0.44 ***
CEC_{eff}	***	*	*	*		*		0.42 ***	-0.22	0.25 *	0.21	-0.03	-0.30 *	0.32 **	0.37 **	0.28 *
BS		***	***	***	***	***	***		-0.91 ***	0.84 ***	-0.72 ***	-0.85 ***	-0.63 ***	-0.40 ***	0.06	0.36 **
Al_{ex}		***	***	***	***	***		***		-0.74 ***	0.71 ***	0.85 ***	0.63 ***	0.46 ***	-0.07	-0.41 ***
Plant a. P		***	***	***	***	***	*	***	***		-0.76 ***	-0.83 ***	-0.54 ***	-0.38 **	0.02	0.35 **
TOC	*	***	***	***	***	***		***	***	***		0.88 ***	0.44 ***	0.66 ***	0.29 *	-0.17
C/N		***	***	***	***	***		***	***	***	***		0.52 ***	0.48 ***	0.03	-0.38 **
Fe_{ox}/Fe_d		***	***	***	***	***	*	***	***	***	***	***		0.37 **	0.02	-0.22
DNA amount	***	***	**	***	***	***	**	***	***	**	***	***	**		0.69 ***	0.26 *
Bacteria	***						**				*			***		0.70 ***
Archaea		**	**	**	*	***	*	**	***	**		**		*	***	

trend existed in the arid and semiarid regions of AZ and SG along the catenas. In the mediterranean climate of LC, the clay content increased significantly from upper slope to lower slope (Fig. 7). The sand contents decreased in the humid climate of NA downslope, whereas the clay content showed an increasing trend with a higher difference of mean values compared to LC (Table 2). No significant differences were found for the BD in all catenas, except of the catena in LC: the south-facing mid slope profile had a significantly lower BD than the upper slope profile (Fig. 7).

In AZ, the high pH values with their overall very low variance (SD 0.1, Table 3) showed no trends between topographic positions. The pH values in SG decreased significantly from upper to mid slope and showed no significant trend along the catenas in LC and NA (Fig. 7). However, the values slightly increased from upper to lower slope in NA.

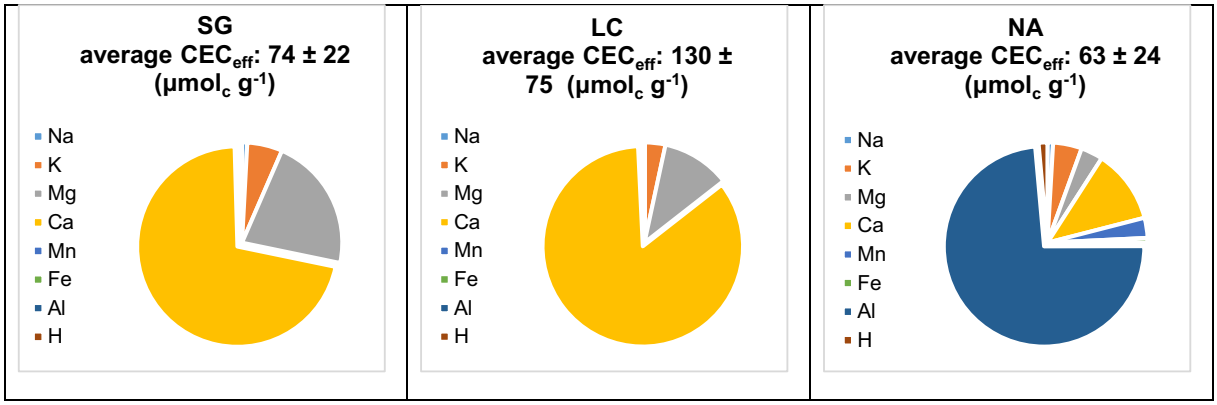

Fig. 5. Contribution of exchangeable cations to the effective cation exchange capacity (CEC_{eff}) of the soil given as average values for 0–40 cm soil depth of the soil profiles at Santa Gracia (SG), La Campana (LC) and Nahuelbuta (NA).

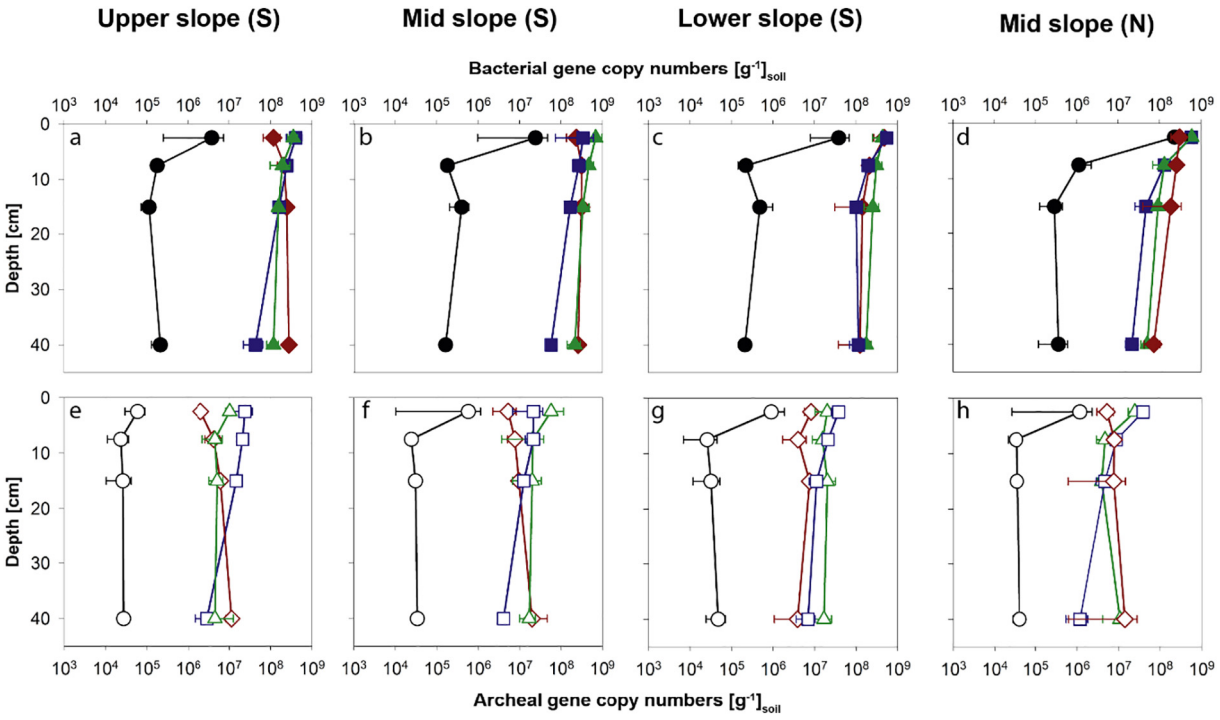

Fig. 6. Abundances of bacterial (full symbols, a–d) and archaeal (open symbols, e–h) 16S rRNA gene copy numbers g-1 soil for Pan de Azúcar (black dots), Santa Gracia (blue squares), La Campana (green triangles) and Nahuelbuta (red diamonds). Data points represent mean abundances of replicate samples, each measured in quadruplicate qPCR reactions, and respective standard deviations (S: south-facing, N: north-facing; cf. Table S4, Bernhard et al., 2018 for original data). (For interpretation of the references to color in this figure legend, the reader is referred to the web version of this article.)

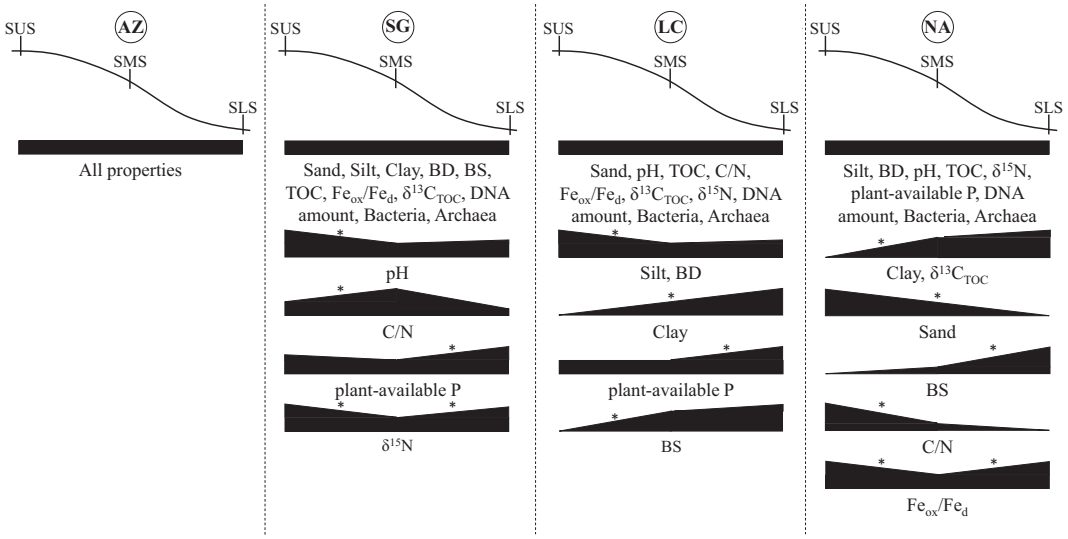

Fig. 7. Trends of physical and chemical soil properties and microbiological variables along the catena of the south-facing slope for each study site. An asterisk indicates significant differences ($p < 0.05$) identified by ANOVA between the profiles within a catena. The different thicknesses of the horizontal bars are arbitrary, but visualize the direction of the trends (cf. Tables S2, S4, Bernhard et al., 2018 for original data).

The pH values and BS are strongly positively correlated (r = 0.85***, Table 4). BS increased significantly from upper to lower slope in LC and NA. The net increase of values was little (0.8) in LC and large (15.2, Table 2) in NA. The TOC did not show significant differences between the topographic positions. Conversely, the $\delta^{13}C_{TOC}$ showed a significant increasing trend from upper to lower slope in NA (Fig. 7).

With regard to DNA concentrations (Fig. 4n) and microbial abundances (Fig. 6a–c and e–g; Table S4, Bernhard et al., 2018), no topographic-specific differences were detected in the south-facing profiles of AZ, SG and LC. Here, bacterial as well as archaeal cell numbers showed decreasing trends from 0 to 40 cm in all slope positions. Only minor topographic-specific variations were observed in the humid site NA. Both, bacterial and archaeal abundances increased with depth in the upper- and mid-slope profile and decreased in the lower-slope profile.

In summary, we found no trend of changes in the physical, chemical and microbiological soil properties along the south-facing slopes of all study sites. Only a few significant differences along the catenas refer to a local heterogeneity along slopes as hypothesized previously.

3.3. Aspect

The clay content at the north-facing mid slope (23.5%) was much

higher in comparison to the south-facing mid slope (7.6%) in SG. This decrease of clay content from the dryer north-facing to the moister south-facing slope in SG is not in concordance with the increasing trend along the regional gradient from semiarid (12.0%) to humid climate (26.1%, Table 3). In contrast, the clay contents in NA increased significantly from north- (24.0%) to south-facing slope (28.7%, Table 2, Fig. 8) corresponding to the climate gradient. For BD, the effect of aspect, i.e. decrease from dryer north-facing slopes to moister south-facing slopes (Table 2), correlated with the regional climate gradient, i.e. increase from semiarid to humid climate (Section 3.2, Fig. 4d). However, the difference was only significant in LC (Fig. 8).

The pH values only decreased significantly from north- to south-facing slope in LC and NA (Table 2, Fig. 8). Thus, the local trend of aspect correlated with the regional climate gradient, but only occurred in mediterranean and humid climate. In general, we did not find significant differences in BS between aspects, except for NA were BS decreased from north- (25.0%) to south-facing slope (11.6%) which also holds true for the regional climate gradient.

The TOC contents were higher on moister south-facing slopes than on dryer north-facing slopes for all study sites, except AZ (Table 2). This relates to the regional climate gradient of increasing TOC with increasing humidity (Section 3.2), but the differences were not significant (Fig. 8). There were no significant differences for C/N ratio between north- and south-facing slopes. The $\delta^{13}C_{TOC}$ were significantly different between slopes in SG, e.g. the north-facing slope (−22.1‰) had a higher mean value compared to the south-facing slope (− 24.5‰, Table 2), but there was no significant difference between slopes in the other study sites (Fig. 8).

DNA concentrations (Fig. 4n) and microbial abundances (Fig. 6; Table S4, Bernhard et al., 2018) did not differ significantly between south-facing and north-facing mid slopes. However, minor variations were detected along the depth profiles. Overall, higher amounts of DNA were extracted from the south-facing mid slopes in all study sites, which correlates to the increase of DNA amount from arid to humid climate conditions. Besides the most arid region AZ, also higher bacterial and archaeal abundances were observed in the south-facing slopes, respectively (Fig. 6b, f). AZ revealed the contrary trend with higher abundances in the north-facing slope (Fig. 6d, h). Along the depth profiles, soil microbial abundances decreased in the south-facing and north-facing mid slopes of AZ, SG and LC. The depth profiles in NA revealed contrary trends by comparison. Here, bacterial and archaeal cell numbers increased in the south-facing slope, whereas cell numbers decreased in the north-facing slope.

In summary, the comparison of the mid slope profiles between north- and south-facing slopes showed no significant trends for most of the physical and chemical soil properties. No aspect-related significant differences of all properties were observed in AZ (Fig. 8). Significant difference were observed for $\delta^{13}C_{TOC}$ and clay content in SG, for silt, BD, pH, Fe_{ox}/Fe_d and plant-available P in LC and for pH and clay content in NA. Since the properties, which show significant differences, are not the same across all study sites, the aspect-related differences represent local heterogeneities rather than a general aspect-related trend along the climate gradient.

4. Discussion

4.1. Climate gradient

4.1.1. Biocrusts

Although many papers on microbial life in the Atacama Desert exist (e.g. Schulze-Makuch et al., 2018, and references therein), biocrusts are still almost unstudied (Wang et al., 2017). Our first results on biocrusts in Chile showed that the climate gradient is strongly reflected in the biocrust type and areal occurrence with a decrease in soil coverage and species of different organization levels from arid to humid regions (Table S6, Bernhard et al., 2018). Also the biocrust community changes from desiccation tolerant lichens in the arid climate to moss and/or liverwort dominated biocrusts in the mediterranean and humid climate of LC and NA. From NA, so far, only early successional biocrusts are known containing green algae associated with few cyanobacteria. Biocrusts in SG consisted of both moss and lichen members. This difference can be explained by the dominant form of atmospheric water supply being a key driver of biocrust community structure - while aero-terrestrial green algae can use water vapor as the only water source, liquid water (rain or dew) is a prerequisite for the development of cyanobacteria (Lange et al., 1986). Particularly filamentous cyanobacteria such as *Nostoc* species represent key organisms for nitrogen fixation, and according to Elbert et al. (2012) biocrusts worldwide contribute to approximately 46% of total global terrestrial biological N-fixation. Filamentous cyanobacteria (*Microcoleus*, *Leptolyngbya* etc.) and filamentous green algae (e.g. *Klebsormidium*) excrete high amounts of sticky exopolysaccharides (EPSs), which interact with soil particles, thereby enhancing soil stability and providing resistance against soil erosion (Garcia-Pichel and Wojciechowski, 2009). In a recent paper, Wang et al. (2017) showed for the Atacama Desert that biocrust sites exhibited thicker soil profiles compared to non-biocrust sites. These authors demonstrated that biocrusts limit wind-driven erosion and promote significant soil accumulation and evolution via the retention of atmospheric deposition resulting in different landscape features.

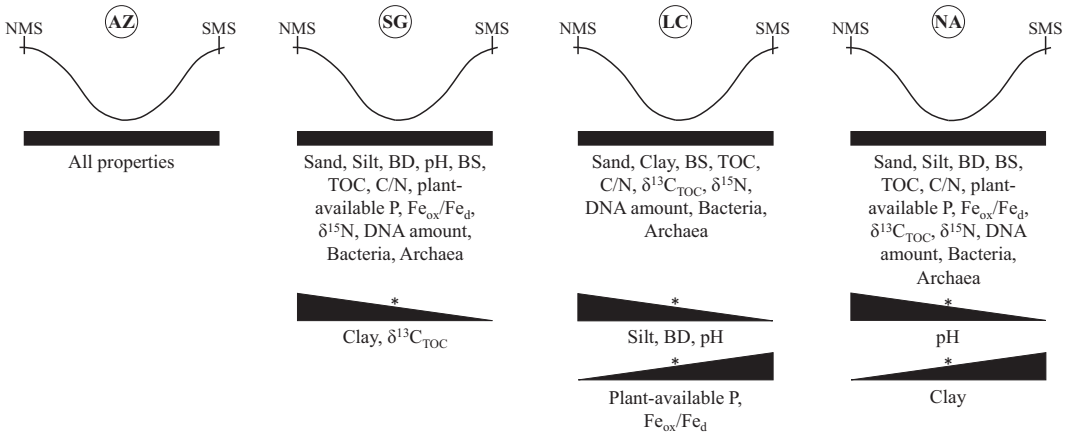

Fig. 8. Trends of physical and chemical soil properties and microbiological variables between north-facing mid slopes (NMS) and south-facing mid slopes (SMS) for each study site. An asterisk indicates significant differences ($p < 0.05$) identified by ANOVA between the profiles. The different thicknesses of the horizontal bars are arbitrary, but visualize the direction of the trends (cf. Tables S2, S4, Bernhard et al., 2018 for original data).

4.1.2. Pedogenesis

The observed increase in soil thickness with increasing precipitation (Fig. 2, Section 3.1.2) suggests a positive correlation between soil development and precipitation amount. The correlation between soil development and precipitation is reflected in almost all physical, chemical and microbiological soil properties investigated (Fig. 4). For example, the depth of the A horizons increased from arid (AZ) to humid (NA) with simultaneously decreasing contents of coarse material > 2 mm. The texture became finer and BD lower with increasing precipitation as well as vegetation cover. An exception from this trend is the arid study site (AZ), which shows a higher variability of sand, silt and clay contents and a lower BD than in the semiarid site (SG). The explanation for the lower BD in the arid site might be the dominance of physical weathering from the presence of gypsum and other soluble salts (Owen et al., 2011). Their volumetric expansion due to atmospheric salt accumulation reduces the BD under these climate conditions (Ewing et al., 2006). The decrease of BD and increase of clay from the semiarid to humid climate correlates with the increase of TOC contents (Table 4). This is explained by a better developed soil structure in combination with the accumulation of organic matter and the close relationship between the BD with the pore size volume, which is in turn dependent on the TOC content and stage of soil development.

The low BD for mineral soils (< 0.8 Mg m^{-3}, Table 2) towards the surface on the south-facing slope in NA might be related to the very dense rooting in the upper horizon (Kodešová et al., 2006). The overall low BD of 0.9 Mg m^{-3} to depths of 60 cm in the humid region (NA) indicates an influence of volcanic ash together with the Al_{ox} + 0.5 Fe_{ox} contents between 0.4% and 2% (Table S2, Bernhard et al., 2018), which are within the range for vitric properties (IUSS Working Group WRB, 2015). However, the second requirement for vitric properties, the occurrence of volcanic glass, glassy aggregates or other glass-coated primary minerals was not indicated for the soils by the Si_{ox}/Al_{ox} ratio, a marker of allophane-like materials, being mainly below 0.5 (Mizota and van Reeuwijk, 1989). In Chile, Umbrisols and also other soils showing andic properties with low BD and high P retention and OM content have been reported for metamorphic rocks without evidence for input of volcanic ashes (Luzio et al., 2001; Luzio, 2011). Matus et al. (2006) found that OM-Al complexes in acid soils are strongly correlated to TOC accumulation, whereas clay contents and hence the associated allophane contents are only poorly correlated. Therefore, we consider that the influence of volcanic ashes is relatively low in this case and assign the high TOC contents together with the low BD mostly to the humid climate and the acid soil. However, a potential influence of volcanic ashes on soil development cannot be finally assessed by our dataset.

The Fe_{ox}/Fe_d ratio generally increases from the arid (AZ) to the humid study site (NA) indicating an increasing activity of pedogenic processes, i.e. formation of amorphous oxides as a result of weathering of primary silicates as described by Baumann et al. (2014). However, the semiarid region SG showed a higher Fe_{ox}/Fe_d ratio than the mediterranean region LC (Fig. 4m). This may be caused by the influence of coastal fog in SG, that contributes with 3.0 L m^2 d^{-1} (El Tofo 29°27′S, 71°18′W) two times more to the water input near SG (El Tofo) than near AZ with 1.4 L m^2 d^{-1} (Falda Verde 26°17′S, 70°36′W; Larrain et al., 2002). Further, the bedrock at SG is more weatherable than that at the other sites, and the degree of weathering is correspondingly higher (Oeser et al., 2018). The higher water availability particularly in the upper part of the soils caused by the coastal fog in SG, which is not present in LC, in conjunction with the more weatherable rock fosters the production of more oxalate soluble iron components that shows a higher pedogenic activity by a higher Fe_{ox}/Fe_d ratio.

4.1.3. Nutrient availability (pH value, CEC_{eff}, plant-available P, C/N, TOC) and isotope composition ($\delta^{13}C_{TOC}$)

A continuous decreasing trend of pH values occurs from the northern arid to southern humid study site (Fig. 4e). The input of atmospheric aerosols, e.g. salts, gypsum and calcium carbonates in northern Chile (Ewing et al., 2006) and the arid climatic conditions with minimal leaching explain the alkaline pH values of around 8 in AZ. The southward increasing precipitation causes leaching of exchangeable base cations, resulting in a lowering of pH values which is particularly visible in NA (Fig. 4e and Fig. 5). Regarding regional climate conditions, the boundary between acid and alkaline soil pH in the absence of calcareous bedrock has been suggested to occur when evapotranspiration equals precipitation (Slessarev et al., 2016). Therefore, alkaline pH values are expected in SG with semiarid climate as well. However, the effect of climate on the pH can be masked by topography and mineralogy (Slessarev et al., 2016). Since we have no topographic gradient from north to south parallel to our climate gradient and we see no clear local effect of topography on soil acidity for any of our study sites, it can be assumed that the granitoid parent material causes the pH values to be below alkaline at the semiarid site. The with depth decreasing pH values within the mediterranean site LC can be explained by ascendant water flow at the end of the long dry period from September to April (Fick and Hijmans, 2017). A threshold region between the mediterranean (LC, 367 mm MAP) and the humid study site (NA, 1469 mm MAP; Table 1) existed for the BS in our dataset (Fig. 4g).

Despite the latitudinal increase in TOC and clay mineral contents that would increase cation-exchange capacity towards the humid study site (NA), the average CEC_{eff} was lowest in NA. This is attributed to the leaching of exchangeable Ca^{2+} and Mg^{2+} due to the high precipitation and acidic pH values (Table 2). Furthermore, Al^{3+} was released from silicate minerals by weathering (Oeser et al., 2018) and became the dominant buffering agent, resulting in a high proportion of Al_{ex} in the CEC_{eff} (> 73% on average, Fig. 5). The leaching of exchangeable base cations like Ca^{2+}, Mg^{2+} and K^+ reflects a pronounced loss of some plant-available nutrients in NA, which creates together with the increased mobility of phytotoxic Al^{3+} a challenging environment for local plants and microorganisms due to their sensitivity to pH values (Lauber et al., 2009). Further, soil acidification and high contents of exchangeable Al^{3+} in 0–40 cm depth (Fig. 4) could lead to restriction of nutrient uptake by biota due to a poor replacement of base cations (Marschner, 1991).

P mostly occurs in the form of Ca-phosphates (apatite) in the arid region AZ with the highest pH of all study sites (8.1). The increase in plant-available P from the arid site AZ to the semiarid site SG resulted from an increased solubilization of apatite with decreasing pH (Smeck, 1985). The generally low concentrations of plant-available P in LC and NA (pH < 6) can be explained by a high proportion of P absorbed to or occluded in pedogenic Fe and Al (hydr-)oxides (Smeck, 1985). This goes along with high concentrations of $(Fe, Al)_{ox}$ and $(Fe, Al)_d$ at NA (Table S2, Bernhard et al., 2018). Also the decreasing pH value in the southern sites promotes P-binding (Sato and Comerford, 2005). In summary, P is easier plant-available in the northern study sites, where vegetation cover is less dense compared to the southern study sites, where plant-available P is lower and the vegetation cover more dense.

TOC contents and C/N ratio (Fig. 4j, k) follow the humidity gradient from north to south and relate to the increasing LAI and, therefore, higher biomass production, given by a higher LAI and vegetation cover (Section 3.1.1). However, according to changes in climate along our gradient, decomposition increases towards the south due to better moisture conditions compared to the continuously or seasonally dry sites further north, as observed in decomposition experiments in the study sites. Furthermore, the dominant trees in the southernmost (i.e. coolest) site NA are broadleaved deciduous *Nothofagus* species, which produce more easily decomposable litter. Therefore, we assume that the higher TOC values in the moister sites are related mostly to higher biomass and litter production, driven by the wetter climate in spite of increased decomposition caused by better water availability. In accordance with the increasing decomposition, the increasing C/N ratio from the northern to southern study sites might also be related to microbial activities, since this ratio is a major driver of microbial processes in soil, such as nutrient mineralization (Delgado-Baquerizo et al.,

2017). The increasing C/N ratios can cause the increase of relative abundances of specific microorganisms (Delgado-Baquerizo et al., 2017), as it is also seen in our study.

The mean $\delta^{13}C_{TOC}$ signature varies across the climate gradient (Table S2, Bernhard et al., 2018), resulting from $\delta^{13}C_{TOC}$ variations between plant species, the relative importance of plant tissues in the litter, as well as direct climate effects on $\delta^{13}C_{TOC}$ discrimination in plants and soil (Acton et al., 2013; Brunn et al., 2014). The higher (less negative) $\delta^{13}C_{TOC}$ values of the semiarid site SG compared to the mediterranean and humid sites (LC and NA), but also to the arid site AZ can be ascribed to the differing plant species of SG, as the in the warm and dry climate of SG dominating plants use C4 (grasses) and Crassulacean-acid metabolism (CAM) photosynthesis (e.g. cacti) with a lower isotopic discrimination against ^{13}C (Ehleringer et al., 1998; O'Leary, 1981; Troughton and Card, 1975). This higher ^{13}C enrichment at SG might (besides the contribution of CAM plants) also partly result from a higher fractionation at the stomata following drought stress in the drier northern ecosystems. However, this effect seems to be minor compared to the plant species as the arid site AZ has similar mean values as the southern more humid sites, but as well a C3 plants dominated vegetation (Table S5, Bernhard et al., 2018). The slightly lower $\delta^{13}C_{TOC}$ in the mediterranean site LC compared to the humid site NA could also be explained by the vegetation species: LC has a very rich herbaceous layer (4–8% lignin) and NA is mainly dominated by woody plants, including conifers, which have a higher amount of the structural macromolecule lignin (17–31%, Benner et al., 1987; Weedon et al., 2009), which is generally ^{13}C-depleted (Benner et al., 1987) and more resistant against microbial decomposition in comparison to hemicellulose and cellulose, hence, it decomposes more slowly (Hedges and Mann (1979). However, Schmidt et al. (2011) recently questioned a longer mean residence time of lignin in soil compared to bulk SOM.

The $\delta^{13}C_{TOC}$ increase with soil depth ($\delta^{13}C_{TOC} \approx 2.0‰$) in SG, LC and NA (Fig. 4l) is common for all soil profiles around the world and can be explained by the following mechanisms: The isotopic fractionation during microbial decomposition of soil organic matter results in a higher ^{13}C-enrichment in more frequently microbial processed organic material than less processed one (Mariotti and Balesdent, 1990) because of the release of isotopically depleted CO_2 (Werth and Kuzyakov, 2010). For instance, Gunina and Kuzyakov (2014) showed strong $\delta^{13}C_{TOC}$ increase in small aggregates and in heavy fractions of organic matter because of intensive microbial processing of these pools. Further, plant litter is generally ^{13}C depleted, while microbial and root biomass is ^{13}C enriched in relation to bulk soil $\delta^{13}C_{TOC}$ (Blagodatskaya et al., 2011; Novara et al., 2014). With increasing soil depth, the proportion of aboveground litter decreases as the proportion of the root biomass increases (Brunn et al., 2014; Garten et al., 2000; Mariotti and Balesdent, 1990). The $\delta^{13}C_{TOC}$ depth trends in NA, LC and SG reflected these mechanisms, but not in AZ. This is due to the missing vegetation cover by higher plants (< 5%) within the arid site.

4.1.4. Microbial abundances

DNA concentrations in the soil (Fig. 4n) showed an increasing trend along the precipitation gradient from AZ to NA and correlate positively with the TOC and C/N ratio (Table 4).

Regarding relative microbial abundances, no clear climatic trend was observed. In all study sites, bacteria numerically outpace archaea, which is typical for soils in many different climatic environments (e.g. Aller and Kemp, 2008; Bengtson et al., 2012). The northern arid site (AZ) displayed significantly lower microbial abundances relative to the other sites, despite the uppermost 5 cm. This is most likely related to the absence of TOC and the alkaline pH (8.3). This harsh life under drought conditions with extreme UV radiation favors only microorganisms that are highly adapted and able to cope with these conditions. The Atacama Desert is considered as an extreme biosphere with a particular diversity of ecological niches (Bull et al., 2016). Detected microbial abundances in AZ are in good accordance with previous studies of the Atacama Desert (e.g. Crits-Christoph et al., 2013; Fletcher et al., 2011; Glavin et al., 2004; Maier et al., 2004; Neilson et al., 2017). However, it has to be considered that we cannot distinguish if the detected gene copies represent active, dormant or dead cells. This question was already discussed in a study by Schulze-Makuch et al. (2018), which used a special DNA-extraction method for distinction. In NA, LC and SG, cell numbers of bacteria as well as archaea have the same range and cluster together. Hence, differences in microbial abundances are most pronounced under arid climate conditions in comparison with semi-arid, mediterranean and humid climate conditions. Bachar et al. (2010) previously reported this trend and detected no significant differences in bacterial abundances between semi-arid and mediterranean soils. Overall, our results suggest that variations in precipitation and temperature have a minor influence on soil bacterial and archaeal abundances in such transect.

In contrast, Bachar et al. (2010) already indicated precipitation as independent factor. Therefore, the soil depth, pH, nutrient availability and organic carbon content might have a greater influence on microbial abundances. Several publications demonstrated the strong effect of soil pH and carbon content on microorganisms (e.g. Bengtson et al., 2012; Bates et al., 2011; Zhou et al., 2002). However, our results do not show these corresponding trends of microbial abundances and physical and chemical soil properties. In general, our results demonstrated a decrease of relative microbial abundances with soil depth by up to three orders of magnitude (Fig. 6). This trend is also continued down to the saprolite, which is shown in Oeser et al. (2018), and in agreement with several publications (e.g. Agnelli et al., 2004; Eilers et al., 2012; Fierer et al., 2003; Will et al., 2010; Blume et al., 2002). Detected microbial abundances are in close relation to the total organic carbon content, which varies positively according to precipitation from semi-arid to humid climate, while microbial cell numbers decreased in the same way (Doetterl et al., 2015). Therefore, it is suggested that soil depth and the TOC content have a more pronounced influence on microbial abundances. Nevertheless, further analyses are needed to obtain a detailed community characterization, since this data only represents relative abundances.

4.2. Catenas

Reference Soil Groups do not vary along the south-facing slope catenas in all study sites. Nonetheless, soil depth varied along the slopes, with a thickening of soil depth towards lower-slope positions under arid and semi-arid climate, and towards mid-slope positions under mediterranean and humid climate. The BD reflects this trend in LC, with 1.3 $Mg\,m^{-3}$ at the upper slope, which is almost the same as the BD of the saprolite (1.4 $Mg\,m^{-3}$), compared to the BD of the mid slope (0.8 $Mg\,m^{-3}$). Generally, a higher thickness of A horizons at lower topographic positions compared to upper slope position within the mediterranean site LC (Fig. 3c) indicates recent soil erosion (i.e. before 1967: LC is National Park since then) along the slopes under mediterranean climate and suggests more intense erosion events in LC compared to the other study sites. This cannot be ascribed to the vegetation cover, being 100% around the investigated soil profiles in LC and the humid site NA (see Section 3.1.1). Another reason for erosion might be related to the occurrence of fire hazards (Grimm et al., 2002), as indicated for LC by the occurrence of charcoal in 0–5 cm depth around the soil pits. These results coincide with a recent erosion study in Chile by Carretier et al. (2018), showing the highest erosion rates within the mediterranean climate region. In addition, downslope transport of clay in the mediterranean and humid sites LC and NA can be related to higher precipitation (Khomo et al., 2011)

Under humid conditions, dissolved ions including base cations can be laterally translocated downslope along the catena (e.g. Sommer and Schlichting, 1997). Along the Coastal Cordillera of Chile, the BS increased significantly downslope in mediterranean and humid climate (Fig. 7; Table S2, Bernhard et al., 2018). This trend did not exist in

semiarid climate in SG (Fig. 7, Table 2), because evapotranspiration exceeds precipitation and leads to ascendant water flow at all topographic positions hampering lateral water flow. In AZ, no water-related transport processes along the slope were indicated by the pH values, reflecting the arid climatic conditions. In addition, the input of marine aerosols with sea salts leading to an unusually high accumulation of salts in soils of Northern Chile (Amundson et al., 2008; Ewing et al., 2006) is most likely similar for the four soil profiles in AZ due to their proximity, supporting the low variability of pH values between topographic positions. The TOC results showed no significant differences between topographic positions in AZ, SG and NA. Therefore, the TOC was not linked to clay transport (i.e. TOC in clay humus complexes) along the slope in the humid site NA contradicting the findings by Khomo et al. (2011), who stated that other soil properties will differ as a consequence of downslope clay transport. The significant shift of heavier $\delta^{13}C_{TOC}$ signatures from upper to lower slope in the humid site NA could be a result of facilitated SOC mineralization, resulting also in higher $\delta^{13}C_{TOC}$ signatures in the moister mid- and lower-slope position compared to the upper slope. All other physical, chemical and microbiological soil properties did not show significant differentiation along the catenas (Fig. 7).

As mentioned in detail above, a large number of significant but non-uniform trends of physical, chemical and microbiological soil properties along the catenas were found for each study site (Fig. 7). This is in good accordance with findings from subtropical forest ecosystems in southeast China (Scholten et al., 2017), showing that individual soil fertility attributes such as base cations are specifically related to terrain attributes.

4.3. Aspect

The aspect of the slope is expected to influence physico-chemical and microbial soil properties, because of differences in radiation and related parameters like evaporation, soil moisture and temperature. In principle, we assume that the differences should have the same trend on a local scale as compared to the regional-climate gradient from the dry northern to the humid southern study site. However, local trends of N-S aspect in concordance with the regional trend become only significant for clay contents in NA, and for pH value in LC and NA (Fig. 8). This leads to the assumption that the effect of aspect to create a local climate gradient with different moisture contents becomes more pronounced with increasing distance to the equator, leading to an increasing difference of sunshine duration on the slopes. The three orders of magnitude higher clay contents on the north-facing slope of the semiarid site SG compared to its south-facing slope suggests that the north-facing slope soil is formed from differing parent material. Oeser et al. (2018) classified the rocks in SG as gabbros and diorites, igneous rocks with low quartz content, but described the surface of the regolith profiles as sub-angular, coarse sand sized quartz and granodiorite fragments. This can lead to a large variety of different properties of the same parent material on short distance.

Furthermore, the vegetation in the north- and south-facing plots differed at all four sites (c.f. Section 3.1.1; Table S5, Bernhard et al., 2018), though this is not necessarily due to the aspect, vegetation being generally heterogenous in the study sites. However, only in SG (Fig. 8) $\delta^{13}C_{TOC}$ values differed clearly between north- and south-facing slopes, with higher ^{13}C enrichment at the north-facing slope. This originates from the dominance of CAM plants on the north-facing slope, in particular the cactus (*Cumulopuntia sphaerica*), and their different photosynthesis, resulting in higher $\delta^{13}C$ values.

Moreover, the slope aspect had only a minor influence on bacterial and archaeal abundances. Excepting the arid site AZ, higher DNA concentrations and abundances (Fig. 6) were detected on the south-facing slope. Microorganisms in AZ favored the north-facing slope, possibly due to temperature conditions. Further, abundances decreased with depth regardless of study site and aspect with one exception in the humid area NA. Here, microbial abundances increased in the south-facing slope, which can be related to the slight increase in pH. With regard to bacterial cell numbers, both trends are also supported by a study by Bardelli et al. (2017).

5. Conclusions

The unique latitudinal gradient in the Coastal Cordillera of Chile documents the effects of the main soil forming factor – climate – on all groups of pedogenic and microbial processes excluding other potentially confounding factors such as differences in parent material. The clay contents, soil depth, Ah horizon depth as well as TOC contents and DNA amounts increased from arid to humid climate, whereas BD, pH values and BS decreased. These parameters were the most prominent indicators of a progressive soil formation with accumulation of organic matter, silicate weathering and accompanying element loss as key pedogenic processes. Further, we found a non-linear relationship of pedogenic and microbial processes in soils depending on climate with a sharp threshold between arid and semi-arid conditions. The arid site differs most with its finer texture and higher BD and alkaline pH values as a result of aeolian deposition and salt precipitation close to the surface. The aeolian deposition is also reflected by a higher areal coverage and a differing composition of biocrusts with a dominance of chlorolichens. This confirms our first hypothesis that soil formation as well as microbial abundances increase with increasing humidity but non-linearity and thresholds along the gradient occur for specific soil properties. Our data show higher local variation in bacterial and archaeal abundances in the arid site. Therefore, we conclude that microorganisms adapt very well to a wide range of climatic conditions, but are challenged under arid climate by the low water availability and extreme UV radiation and hence have to be highly specialized.

We can also partly confirm our second hypothesis that a local gradient of soil properties exist along the catena, but is minor compared to the steep regional climate gradient. However, characteristic processes such as leaching, transport of cations and clay downslope along the catenas were only significant under mediterranean and humid climate in the southernmost part of the latitudinal gradient. These processes are absent under arid conditions. Therefore, we conclude that individual physico-chemical and microbial soil properties on local scale are specifically related to terrain attributes or small-scale heterogeneities on slopes rather than to soil erosion or the downslope increase in soil moisture. Reasons could be the limited length of our catenas and the unknown effects of vegetation types, litter or biocrust cover and terrain on soil erosion.

The N-S aspect and microclimate effects (our 3rd hypothesis) were observed only under the semiarid, mediterranean and humid climate for differing parameters like texture, pH value, BD, plant-available P or $\delta^{13}C_{TOC}$ values, but not for microbial abundances. The local variability in soil and microbiological parameters overall exceeds a possible microscale climate effect of the different aspects. Especially in the dryer north aspect effects are not detectable, most likely due to a high zenith angle in proximity to the equator, leading to a minimal difference of sunshine duration between slopes.

Finally, we showed that the dependency of pedogenesis and soil microbial abundances on climate and topography can be untangled methodologically when climate and topographic gradients cut across and are analyzed at appropriate scales, including the regional scale for climate and the local scale for topography.

Competing interests

The authors declare that they have no conflict of interest.

Acknowledgements

We acknowledge support from the German Science Foundation

(DFG) priority program SPP-1803 “EarthShape: Earth Surface Shaping by Biota”. We are grateful to the Chilean National Park Service (CONAF) for providing access to the sample locations (Pan de Azúcar, La Campana and Nahuelbuta) and on-site support of our research. We also thank CEAZA and “Sucesión Gálvez Muñoz”, for providing access to the Reserva Natural Santa Gracia. We also express our deep gratitude to all students and other colleagues, who helped in the field and with logistics during several months of field work and all students and technical assistants in all laboratories, who helped with the analyses.

References

Acton, P., Fox, J., Campbell, E., Rowe, H., Wilkinson, M., 2013. Carbon isotopes for estimating soil decomposition and physical mixing in well-drained forest soils. J. Geophys. Res. Biogeosci. 118 (4), 1532–1545. http://dx.doi.org/10.1002/2013JG002400.

Agnelli, A., Ascher, J., Corti, G., Ceccherini, M.T., Nannipieri, P., Pietramellara, G., 2004. Distribution of microbial communities in a forest soil profile investigated by microbial biomass, soil respiration and DGGE of total and extracellular DNA. Soil Biol. Biochem. 36 (5), 859–868. http://dx.doi.org/10.1016/j.soilbio.2004.02.004.

Aller, J.Y., Kemp, P.F., 2008. Are Archaea inherently less diverse than Bacteria in the same environments? FEMS Microbiol. Ecol. 65 (1), 74–87. http://dx.doi.org/10.1111/j.1574-6941.2008.00498.x.

Amundson, R., Richter, D.D., Humphreys, G.S., Jobbagy, E.G., Gaillardet, J., 2007. Coupling between biota and earth materials in the critical zone. Elements 3 (5), 327–332. http://dx.doi.org/10.2113/gselements.3.5.327.

Amundson, R., Ewing, S., Dietrich, W., Sutter, B., Owen, J., Chadwick, O., Nishiizumi, K., Walvoord, M., McKay, C., 2008. On the in situ aqueous alteration of soils on Mars. Geochim. Cosmochim. Acta 72 (15), 3845–3864. http://dx.doi.org/10.1016/j.gca.2008.04.038.

Amundson, R., Heimsath, A., Owen, J., Yoo, K., Dietrich, W.E., 2015. Hillslope soils and vegetation. Geomorphology 234, 122–132. http://dx.doi.org/10.1016/j.geomorph.2014.12.031.

Bachar, A., Al-Ashhab, A., Soares, M.I.M., Sklarz, M.Y., Angel, R., Ungar, E.D., Gillor, O., 2010. Soil microbial abundance and diversity along a low precipitation gradient. Microb. Ecol. 60 (2), 453–461. http://dx.doi.org/10.1007/s00248-010-9727-1.

Barbosa, W.R., Romero, R.E., de Souza Júnior, Valdomiro Severino, Cooper, M., Sartor, L.R., de Moya Partiti, C.S., Jorge, F.d.O., Cohen, R., de Jesus, S.L., Ferreira, T.O., 2015. Effects of slope orientation on pedogenesis of altimontane soils from the Brazilian semi-arid region (Baturité massif, Ceará). Environ. Earth Sci. 73 (7), 3731–3743. http://dx.doi.org/10.1007/s12665-014-3660-4.

Bardelli, T., Gómez-Brandón, M., Ascher-Jenull, J., Fornasier, F., Arfaioli, P., Francioli, D., Egli, M., Sartori, G., Insam, H., Pietramellara, G., 2017. Effects of slope exposure on soil physico-chemical and microbiological properties along an altitudinal climosequence in the Italian alps. Sci. Total Environ. 575, 1041–1055. http://dx.doi.org/10.1016/j.scitotenv.2016.09.176.

Bates, S.T., Berg-Lyons, D., Caporaso, J.G., Walters, W.A., Knight, R., Fierer, N., 2011. Examining the global distribution of dominant archaeal populations in soil. ISME J. 5 (5), 908–917. http://dx.doi.org/10.1038/ismej.2010.171.

Baumann, F., Schmidt, K., Dörfer, C., He, J.-S., Scholten, T., Kühn, P., 2014. Pedogenesis, permafrost, substrate and topography: plot and landscape scale interrelations of weathering processes on the central-eastern Tibetan Plateau. Geoderma 226-227, 300–316. http://dx.doi.org/10.1016/j.geoderma.2014.02.019.

Bengtson, P., Sterngren, A.E., Rousk, J., 2012. Archaeal abundance across a pH gradient in an arable soil and its relationship to bacterial and fungal growth rates. Appl. Environ. Microbiol. 78 (16), 5906–5911. http://dx.doi.org/10.1128/AEM.01476-12.

Benner, R., Fogel, M.L., Sprague, E.K., Hodson, R.E., 1987. Depletion of 13C in lignin and its implications for stable carbon isotope studies. Nature 329 (6141), 708–710. http://dx.doi.org/10.1038/329708a0.

Bernhard, N., Moskwa, L.-M., Schmidt, K., Oeser, R.A., Aburto, F., Bader, M.Y., Baumann, K., von Blanckenburg, F., Boy, J., van den Brink, L., Brucker, E., Büdel, B., Canessa, R., Dippold, M.A., Ehlers, T.A., Fuentes, J.P., Godoy, R., Jung, P., Karsten, U., Köster, M., Kuzyakov, Y., Leinweber, P., Neidhardt, H., Matus, F., Mueller, C.W., Oelmann, Y., Oses, R., Osses, P., Paulino, L., Samolov, E., Schaller, M., Schmid, M., Spielvogel, S., Spohn, M., Stock, S., Stroncik, N., Tielbörger, K., Übernickel, K., Scholten, T., Seguel, O., Wagner, D., Kühn, P., 2018. Data supplement to “Pedogenic and microbial interrelations to regional climate and local topography: New insights from a climate gradient (arid to humid) along the Coastal Cordillera of Chile”. In: GFZ Data Services, http://dx.doi.org/10.5880/GFZ.5.3.2018.001.

Blagodatskaya, E., Yuyukina, T., Blagodatsky, S., Kuzyakov, Y., 2011. Three-source-partitioning of microbial biomass and of CO2 efflux from soil to evaluate mechanisms of priming effects. Soil Biol. Biochem. 43 (4), 778–786. http://dx.doi.org/10.1016/j.soilbio.2010.12.011.

Blume, E., Bischoff, M., Reichert, J.M., Moorman, T., Konopka, A., Turco, R.F., 2002. Surface and subsurface microbial biomass, community structure and metabolic activity as a function of soil depth and season. Appl. Soil Ecol. 20 (3), 171–181. http://dx.doi.org/10.1016/S0929-1393(02)00025-2.

Blume, H.-P., Stahr, K., Leinweber, P., 2011. Bodenkundliches Praktikum: Eine Einführung in pedologisches Arbeiten für Ökologen, insbesondere Land- und Forstwirte, und für Geowissenschaftler, 3., neubearb. Aufl. ed. Spektrum Akademischer Verlag, Heidelberg (255 pp).

Bojko, O., Kabala, C., 2016. Transformation of physicochemical soil properties along a mountain slope due to land management and climate changes — a case study from the Karkonosze Mountains, SW Poland. Catena 140, 43–54. http://dx.doi.org/10.1016/j.catena.2016.01.015.

Bojko, O., Kabala, C., 2017. Organic carbon pools in mountain soils — sources of variability and predicted changes in relation to climate and land use changes. Catena 149, 209–220. http://dx.doi.org/10.1016/j.catena.2016.09.022.

Bray, R.H., Kurtz, L.T., 1945. Determination of total, organic, and available forms of phosphorus in soils. Soil Sci. 59 (1), 39–46. http://dx.doi.org/10.1097/00010694-194501000-00006.

Brunn, M., Spielvogel, S., Sauer, T., Oelmann, Y., 2014. Temperature and precipitation effects on δ13C depth profiles in SOM under temperate beech forests. Geoderma 235-236, 146–153. http://dx.doi.org/10.1016/j.geoderma.2014.07.007.

Bull, A.T., Asenjo, J.A., Goodfellow, M., Gómez-Silva, B., 2016. The Atacama desert: technical resources and the growing importance of novel microbial diversity. Annu. Rev. Microbiol. 70, 215–234. http://dx.doi.org/10.1146/annurev-micro-102215-095236.

Carletti, P., Vendramin, E., Pizzeghello, D., Concheri, G., Zanella, A., Nardi, S., Squartini, A., 2009. Soil humic compounds and microbial communities in six spruce forests as function of parent material, slope aspect and stand age. Plant Soil 315 (1–2), 47–65. http://dx.doi.org/10.1007/s11104-008-9732-z.

Carretier, S., Tolorza, V., Regard, V., Aguilar, G., Bermúdez, M.A., Martinod, J., Guyot, J.-L., Hérail, G., Riquelme, R., 2018. Review of erosion dynamics along the major N-S climatic gradient in Chile and perspectives. Geomorphology 300, 45–68. http://dx.doi.org/10.1016/j.geomorph.2017.10.016.

Casanova, M., Salazar, O., Seguel, O., Luzio, W., 2013. The soils of Chile. In: Springer Science + Business Media Dordrecht 2013. Springer, Dordrecht Heidelberg New York London (193 pp).

Chadwick, O.A., Gavenda, R.T., Kelly, E.F., Ziegler, K., Olson, C.G., Elliott, W.C., Hendricks, D.M., 2003. The impact of climate on the biogeochemical functioning of volcanic soils. Chem. Geol. 202 (3–4), 195–223. http://dx.doi.org/10.1016/j.chemgeo.2002.09.001.

Cleveland, W.S., Grosse, E., Shyu, M., 1992. Local regression models. In: Chambers, J.M., Hastie, T.J. (Eds.), Statistical Models in S. Wadsworth & Brooks, Cole, pp. 309–376.

Crits-Christoph, A., Robinson, C.K., Barnum, T., Fricke, W.F., Davila, A.F., Jedynak, B., McKay, C.P., Diruggiero, J., 2013. Colonization patterns of soil microbial communities in the Atacama Desert. Microbiome 1 (1), 28. http://dx.doi.org/10.1186/2049-2618-1-28.

Delgado-Baquerizo, M., Reich, P.B., Khachane, A.N., Campbell, C.D., Thomas, N., Freitag, T.E., Abu Al-Soud, W., Sørensen, S., Bardgett, R.D., Singh, B.K., 2017. It is elemental: soil nutrient stoichiometry drives bacterial diversity. Environ. Microbiol. 19 (3), 1176–1188. http://dx.doi.org/10.1111/1462-2920.13642.

Doetterl, S., Stevens, A., Six, J., Merckx, R., van Oost, K., Casanova Pinto, M., Casanova-Katny, A., Muñoz, C., Boudin, M., Zagal Venegas, E., Boeckx, P., 2015. Soil carbon storage controlled by interactions between geochemistry and climate. Nat. Geosci. 8 (10), 780–783. http://dx.doi.org/10.1038/ngeo2516.

Egli, M., Mirabella, A., Sartori, G., Zanelli, R., Bischof, S., 2006. Effect of north and south exposure on weathering rates and clay mineral formation in Alpine soils. Catena 67 (3), 155–174. http://dx.doi.org/10.1016/j.catena.2006.02.010.

Ehleringer, J.R., Rundel, P.W., Palma, B., Mooney, H.A., 1998. Carbon isotope ratios of Atacama Desert plants reflect hyperaridity of region in northern Chile. Rev. Chil. Hist. Nat. 71, 19–86.

Eilers, K.G., Debenport, S., Anderson, S., Fierer, N., 2012. Digging deeper to find unique microbial communities: the strong effect of depth on the structure of bacterial and archaeal communities in soil. Soil Biol. Biochem. 50, 58–65. http://dx.doi.org/10.1016/j.soilbio.2012.03.011.

Elbert, W., Weber, B., Burrows, S., Steinkamp, J., Büdel, B., Andreae, M.O., Pöschl, U., 2012. Contribution of cryptogamic covers to the global cycles of carbon and nitrogen. Nat. Geosci. 5 (7), 459–462. http://dx.doi.org/10.1038/ngeo1486.

Ewing, S.A., Sutter, B., Owen, J., Nishiizumi, K., Sharp, W., Cliff, S.S., Perry, K., Dietrich, W., McKay, C.P., Amundson, R., 2006. A threshold in soil formation at Earth's arid–hyperarid transition. Geochim. Cosmochim. Acta 70 (21), 5293–5322. http://dx.doi.org/10.1016/j.gca.2006.08.020.

Fick, S.E., Hijmans, R.J., 2017. WorldClim 2: new 1-km spatial resolution climate surfaces for global land areas. Int. J. Climatol. 37 (12), 4302–4315. http://dx.doi.org/10.1002/joc.5086.

Fierer, N., Schimel, J.P., Holden, P.A., 2003. Variations in microbial community composition through two soil depth profiles. Soil Biol. Biochem. 35 (1), 167–176. http://dx.doi.org/10.1016/S0038-0717(02)00251-1.

Fierer, N., Bradford, M.A., Jackson, R.B., 2007. Toward an ecological classification of soil bacteria. Ecology 88 (6), 1354–1364. http://dx.doi.org/10.1890/05-1839.

Fierer, N., Leff, J.W., Adams, B.J., Nielsen, U.N., Bates, S.T., Lauber, C.L., Owens, S., Gilbert, J.A., Wall, D.H., Caporaso, J.G., 2012. Cross-biome metagenomic analyses of soil microbial communities and their functional attributes. Proc. Natl. Acad. Sci. U. S. A. 109 (52), 21390–21395. http://dx.doi.org/10.1073/pnas.1215210110.

Fletcher, L.E., Conley, C.A., Valdivia-Silva, J.E., Perez-Montaño, S., Condori-Apaza, R., Kovacs, G.T.A., Glavin, D.P., McKay, C.P., 2011. Determination of low bacterial concentrations in hyperarid Atacama soils: comparison of biochemical and microscopy methods with real-time quantitative PCR. Can. J. Microbiol. 57 (11), 953–963. http://dx.doi.org/10.1139/w11-091.

Food and Agriculture Organization of the United Nations (FAO), 2006. Guidelines for Soil Description, 4th ed. Food and Agriculture Organization of the United Nations, Rome (97 pp).

Fox, J., Bouchet-Valat, M., 2017. Rcmdr: R Commander. R Package Version 2.3-2.

Fox, J., Weisberg, S., 2011. An {R} Companion to Applied Regression, Second edition. Sage. URL, Thousand Oaks CA. http://socserv.socsci.mcmaster.ca/jfox/Books/Companion.

Gantner, S., Andersson, A.F., Alonso-Sáez, L., Bertilsson, S., 2011. Novel primers for 16S rRNA-based archaeal community analyses in environmental samples. J. Microbiol. Methods 84 (1), 12–18. http://dx.doi.org/10.1016/j.mimet.2010.10.001.

Garcia-Pichel, F., Wojciechowski, M.F., 2009. The evolution of a capacity to build supracellular ropes enabled filamentous cyanobacteria to colonize highly erodible substrates. PLoS One 4 (11), e7801. http://dx.doi.org/10.1371/journal.pone.0007801.

Gardi, C., Angelini, M., Barceló, S., Comerma, J., Cruz Gaistardo, C., Encina Rojas, A., Jones, A., Krasilnikov, P., Mendonça Santos Brefin, M.L., Montanarella, L., Muñiz Ugarte, O., Schad, P., Vara Rodríguez, M.I., Vargas, R., Ravina da Silva, M., 2015. Soil Atlas of Latin America and the Caribbean. Publications Office of the European Union, L-2995 Luxembourg (176 pp).

Garreaud, R.D., Vuille, M., Compagnucci, R., Marengo, J., 2009. Present-day South American climate. Palaeogeogr. Palaeoclimatol. Palaeoecol. 281 (3–4), 180–195. http://dx.doi.org/10.1016/j.palaeo.2007.10.032.

Garten, C.T., Cooper, L.W., Post, W.M., Hanson, P.J., 2000. Climate controls on forest soil C isotope ratios in the southern Appalachian Mountains. Ecology 81 (4), 1108–1119. http://dx.doi.org/10.1890/0012-9658(2000)081[1108:CCOFSC]2.0.CO;2.

Glavin, D.P., Cleaves, H.J., Schubert, M., Aubrey, A., Bada, J.L., 2004. New method for estimating bacterial cell abundances in natural samples by use of sublimation. Appl. Environ. Microbiol. 70 (10), 5923–5928. http://dx.doi.org/10.1128/AEM.70.10.5923-5928.2004.

Glinka, K.D., 1927. Dokuchaiev's Ideas in the Development of Pedology and Cognate Sciences. The Academy, Leningrad.

Goberna, M., Insam, H., Klammer, S., Pascual, J.A., Sánchez, J., 2005. Microbial community structure at different depths in disturbed and undisturbed semiarid Mediterranean forest soils. Microb. Ecol. 50 (3), 315–326. http://dx.doi.org/10.1007/s00248-005-0177-0.

Goldfarb, K.C., Karaoz, U., Hanson, C.A., Santee, C.A., Bradford, M.A., Treseder, K.K., Wallenstein, M.D., Brodie, E.L., 2011. Differential growth responses of soil bacterial taxa to carbon substrates of varying chemical recalcitrance. Front. Microbiol. 2, 94. http://dx.doi.org/10.3389/fmicb.2011.00094.

Gómez-Brandón, M., Ascher-Jenull, J., Bardelli, T., Fornasier, F., Fravolini, G., Arfaioli, P., Ceccherini, M.T., Pietramellara, G., Lamorski, K., Sławiński, C., Bertoldi, D., Egli, M., Cherubini, P., Insam, H., 2017. Physico-chemical and microbiological evidence of exposure effects on *Picea abies* – coarse woody debris at different stages of decay. For. Ecol. Manag. 391, 376–389. http://dx.doi.org/10.1016/j.foreco.2017.02.033.

Grimm, M., Jones, R., Montanarella, L., 2002. Soil Erosion Risk in Europe. European Commission, Institute for Environment and Sustainability, European Soil Bureau.

Gunina, A., Kuzyakov, Y., 2014. Pathways of litter C by formation of aggregates and SOM density fractions: implications from 13C natural abundance. Soil Biol. Biochem. 71, 95–104. http://dx.doi.org/10.1016/j.soilbio.2014.01.011.

Harrell, F.E.J., Dupont, C., 2017. Hmisc: Harrell miscellaneous. R package version 4.0-3. https://CRAN.R-project.org/package=Hmisc.

Hedges, J.I., Mann, D.C., 1979. The characterization of plant tissues by their lignin oxidation products. Geochim. Cosmochim. Acta 43 (11), 1803–1807. http://dx.doi.org/10.1016/0016-7037(79)90028-0.

Hervé, F., Faundez, F., Calderón, M., Massonne, H.-J., Willner, A.P., 2007. Metamorphic and plutonic basement complexes. In: Moreno, T., Gibbons, W. (Eds.), The Geology of Chile. Geological Soc, London, pp. 5–19.

Hilgard, E.W., 1914. Soils: Their Formation, Properties, Compositions and Relations to Climate and Plant Growth in the Humid and Arid Regions. 19 The Macmillan Company, New York.

Hulton, N.R.J., Purves, R.S., McCulloch, R.D., Sugden, D.E., Bentley, M.J., 2002. The Last Glacial Maximum and deglaciation in southern South America. Quat. Sci. Rev. 21 (1–3), 233–241. http://dx.doi.org/10.1016/S0277-3791(01)00103-2.

IUSS Working Group WRB, 2015. World Reference Base for Soil Resources 2014: International Soil Classification System for Naming Soils and Creating Legends for Soil Maps. Update 2015. World Soil Resources Reports 106, Rome. (191 pp).

Jenny, H., 1994. Factors of Soil Formation: A System of Quantitative Pedology (unabridged, unaltered republ., new foreword ed). Dover Publ, New York (281 pp).

Jungers, M.C., Heimsath, A.M., Amundson, R., Balco, G., Shuster, D., Chong, G., 2013. Active erosion–deposition cycles in the hyperarid Atacama Desert of Northern Chile. Earth Planet. Sci. Lett. 371-372, 125–133. http://dx.doi.org/10.1016/j.epsl.2013.04.005.

Khomo, L., Hartshorn, A.S., Rogers, K.H., Chadwick, O.A., 2011. Impact of rainfall and topography on the distribution of clays and major cations in granitic catenas of southern Africa. Catena 87 (1), 119–128. http://dx.doi.org/10.1016/j.catena.2011.05.017.

Khormali, F., Ghergherechi, S., Kehl, M., Ayoubi, S., 2012. Soil formation in loess-derived soils along a subhumid to humid climate gradient, Northeastern Iran. Geoderma 179-180, 113–122. http://dx.doi.org/10.1016/j.geoderma.2012.02.002.

Kodešová, R., Kodeš, V., Žigová, A., Šimůnek, J., 2006. Impact of plant roots and soil organisms on soil micromorphology and hydraulic properties. Biol. Bratislava 61 (19), 339–343.

Kurtz, L.T., 1942. Elimination of Fluoride Interference in Molybdenum Blue Reaction. Ind. Eng. Chem. Anal. Ed. 14 (11), 855-855.

Lange, O.L., Kilian, E., Ziegler, H., 1986. Water vapor uptake and photosynthesis of lichens: performance differences in species with green and blue-green algae as phycobionts. Oecologica 71 (1), 104–110. http://dx.doi.org/10.1007/BF00377327.

Larrain, H., Velásquez, F., Cereceda, P., Espejo, R., Pinto, R., Osses, P., Schemenauer, R.S., 2002. Fog measurements at the site “Falda Verde” north of Chañaral compared with other fog stations of Chile. Atmos. Res. 64 (1–4), 273–284. http://dx.doi.org/10.1016/S0169-8095(02)00098-4.

Lauber, C.L., Hamady, M., Knight, R., Fierer, N., 2009. Soil pH as a predictor of soil bacterial community structure at the continental scale: a pyrosequencing-based assessment. Appl. Environ. Microbiol. 75 (15), 5111–5120. http://dx.doi.org/10.1128/AEM.00335-09.

Lin, H., 2010. Earth's Critical Zone and hydropedology: concepts, characteristics, and advances. Hydrol. Earth Syst. Sci. 14, 25–45.

Lüer, B., Böhmer, A., 2000. Vergleich zwischen Perkolation und Extraktion mit 1 M NH4Cl Lösung zur Bestimmung der effektiven Kationenaustauschkapazität (KAKeff) von Böden. J. Plant Nutr. Soil Sci. 163 (5), 555–557. http://dx.doi.org/10.1002/1522-2624(200010)163:5<555:AID-JPLN555>3.0.CO;2-#.

Luzio, W., 2011. Suelos de Chile. Maval Impresores, Santiago, Chile. (364 p).

Luzio, W., Sadzawka, A., Besoaín, E., Lara, P., 2001. Inceptisoles de la cordiellera de la costa en la X Región (40°15'–41°00'S) de Chile. Rev. Cien. Suelo Nutr. Veg. 1 (2), 1–16.

Maier, R.M., Drees, K.P., Neilson, J.W., Henderson, D.A., Quade, J., Betancourt, J.L., 2004. Microbial life in the Atacama Desert. Science (New York, N.Y.) 306 (5700), 1289–1290. http://dx.doi.org/10.1126/science.306.5700.1289c.

Mariotti, A., Balesdent, J., 1990. 13C natural abundance as a tracer of soil organic matter turnover and paleoenvironment dynamics. Chem. Geol. 84 (1–4), 217–219. http://dx.doi.org/10.1016/0009-2541(90)90218-V.

Marschner, H., 1991. Mechanisms of adaptation of plants to acid soils. In: Wright, R.J., Baligar, V.C., Murrmann, R.P. (Eds.), Plant-Soil Interactions at Low pH. Springer Netherlands, Dordrecht, pp. 683–702.

Matus, F., Amigo, X., Kristiansen, S.M., 2006. Aluminium stabilization controls organic carbon levels in Chilean volcanic soils. Geoderma 132 (1–2), 158–168. http://dx.doi.org/10.1016/j.geoderma.2005.05.005.

Mehra, O.P., Jackson, M.L., 1958. Iron Oxide Removal From Soils and Clays by a Dithionite-Citrate System Buffered With Sodium Bicarbonate. pp. 317–327.

Milne, G., 1935. Some suggested units of classification and mapping particularly for East African soils. Soil Res. 4, 183–198.

Mizota, C., van Reeuwijk, L.P., 1989. Clay mineralogy and chemistry of soil formed in volcanic materials in diverse climatic regions. In: Soil Monograph. 2 (Wageningen, 194 pp).

Muñoz, J.F., Fernández, B., Varas, E., Pastén, P., Gómez, D., Rengifo, P., Muñoz, J., Atenas, M., Jofré, J.C., 2007. Chilean water resources. In: Moreno, T., Gibbons, W. (Eds.), The Geology of Chile. Geological Soc, London, pp. 215–230.

Murphy, J., Riley, J.P., 1962. A modified single solution method for the determination of phosphate in natural waters. Anal. Chim. Acta 27, 31–36. http://dx.doi.org/10.1016/S0003-2670(00)88444-5.

Mutz, S.G., Ehlers, T.A., Werner, M., Lohmann, G., Stepanek, C., Li, J., 2018. Estimates of late Cenozoic climate change relevant to Earth surface processes in tectonically active orogens. Earth Surf. Dyn. 6 (2), 271–301. http://dx.doi.org/10.5194/esurf-6-271-2018.

Muyzer, G., de Waal, E.C., Uitterlinden, A.G., 1993. Profiling of complex microbial populations by denaturing gradient gel electrophoresis analysis of polymerase chain reaction-amplified genes coding for 16S rRNA. Appl. Environ. Microbiol. 59, 695–700.

Neilson, J.W., Califf, K., Cardona, C., Copeland, A., van Treuren, W., Josephson, K.L., Knight, R., Gilbert, J.A., Quade, J., Caporaso, J.G., Maier, R.M., 2017. Significant impacts of increasing aridity on the arid soil microbiome. mSystems 2 (3). http://dx.doi.org/10.1128/mSystems.00195-16.

Novara, A., La Mantia, T., Rühl, J., Badalucco, L., Kuzyakov, Y., Gristina, L., Laudicina, V.A., 2014. Dynamics of soil organic carbon pools after agricultural abandonment. Geoderma 235-236, 191–198. http://dx.doi.org/10.1016/j.geoderma.2014.07.015.

Oeser, R.A., Stroncik, N., Moskwa, L.M., Bernhard, N., Schaller, M., Canessa, R., van den Brink, L., Köster, M., Brucker, E., Stock, S., Fuentes, J.P., Godoy, R., Matus, F.J., Pedraza, R.O., McIntyre, P.O., Paulino, L., Seguel, O., Bader, M.Y., Boy, J., Dippold, M.A., Ehlers, T.A., Kühn, P., Kuzyakov, Y., Leinweber, P., Scholten, T., Spielvogel, S., Spohn, M., Übernickel, K., Tielbörger, K., Wagner, D., von Blanckenburg, F., 2018. Chemistry and microbiology of the critical zone along a steep climate and vegetation gradient in the Chilean Coastal Cordillera. Catena 170, 183–203. http://dx.doi.org/10.1016/j.catena.2018.06.002.

O'Leary, M.H., 1981. Carbon isotope fractionation in plants. Phytochemistry 20 (4), 553–567. http://dx.doi.org/10.1016/0031-9422(81)85134-5.

Ollivier, J., Yang, S., Dörfer, C., Welzl, G., Kühn, P., Scholten, T., Wagner, D., Schloter, M., 2014. Bacterial community structure in soils of the Tibetan Plateau affected by discontinuous permafrost or seasonal freezing. Biol. Fertil. Soils 50 (3), 555–559. http://dx.doi.org/10.1007/s00374-013-0869-4.

Owen, J.J., Amundson, R., Dietrich, W.E., Nishiizumi, K., Sutter, B., Chong, G., 2011. The sensitivity of hillslope bedrock erosion to precipitation. Earth Surf. Process. Landf. 36 (1), 117–135. http://dx.doi.org/10.1002/esp.2083.

Pankhurst, R.J., Hervé, F., 2007. Introduction and overview. In: Moreno, T., Gibbons, W. (Eds.), The Geology of Chile. Geological Soc, London, pp. 1–4.

Parada, M.A., López-Escobar, L., Oliveros, V., Fuentes, F., Morata, D., Calderón, M., Aguirre, L., Féraud, G., Espinosa, F., Moreno, H., Figueroa, O., Muñoz Bravo, J., Troncoso Vásquez, R., Stern, C.R., 2007. Andean magmatism. In: Moreno, T., Gibbons, W. (Eds.), The Geology of Chile. Geological Soc, London, pp. 115–146.

Pastalkova, H., Podrazsky, V., Vacek, S., 2001. Soils in the dwarf pine altitudinal zone of the Giant Mts. Opera Corcontica 38, 207–217.

Pizarro, R., Valdés, R., García-Chevesich, P., Vallejos, C., Sangüesa, C., Morales, C., Balocchi, F., Abarza, A., Fuentes, R., 2012. Latitudinal analysis of rainfall intensity and mean annual precipitation in Chile. Chil. J. Agric. Res. 72 (2), 252–261. http://dx.doi.org/10.4067/S0718-58392012000200014.

R Core Team, 2017. R: A Language and Environment for Statistical Computing. R Foundation for Statistical Computing, Vienna, Austria. URL. https://www.R-project.org/.

Raheb, A., Heidari, A., Mahmoodi, S., 2017. Organic and inorganic carbon storage in soils along an arid to dry sub-humid climosequence in northwest of Iran. Catena 153, 66–74. http://dx.doi.org/10.1016/j.catena.2017.01.035.

Sato, S., Comerford, N.B., 2005. Influence of soil pH on inorganic phosphorus sorption and desorption in a humid Brazilian ultisol. Rev. Bras. Ciênc. Solo 29 (5), 685–694. http://dx.doi.org/10.1590/S0100-06832005000500004.

Schmidt, M.W.I., Torn, M.S., Abiven, S., Dittmar, T., Guggenberger, G., Janssens, I.A., Kleber, M., Kögel-Knabner, I., Lehmann, J., Manning, D.A.C., Nannipieri, P., Rasse, D.P., Weiner, S., Trumbore, S.E., 2011. Persistence of soil organic matter as an ecosystem property. Nature 478 (7367), 49–56. http://dx.doi.org/10.1038/nature10386.

Scholten, T., Goebes, P., Kühn, P., Seitz, S., Assmann, T., Bauhus, J., Bruelheide, H., Buscot, F., Erfmeier, A., Fischer, M., Härdtle, W., He, J.-S., Ma, K., Niklaus, P.A., Scherer-Lorenzen, M., Schmid, B., Shi, X., Song, Z., von Oheimb, G., Wirth, C., Wubet, T., Schmidt, K., 2017. On the combined effect of soil fertility and topography on tree growth in subtropical forest ecosystems—a study from SE China. J. Plant Ecol. 10 (1), 111–127. http://dx.doi.org/10.1093/jpe/rtw065.

Schulz, K., Mikhailyuk, T., Dreßler, M., Leinweber, P., Karsten, U., 2016. Biological soil crusts from coastal dunes at the Baltic Sea: cyanobacterial and algal biodiversity and related soil properties. Microb. Ecol. 71 (1), 178–193. http://dx.doi.org/10.1007/s00248-015-0691-7.

Schulze-Makuch, D., Wagner, D., Kounaves, S.P., Mangelsdorf, K., Devine, K.G., de Vera, J.-P., Schmitt-Kopplin, P., Grossart, H.-P., Parro, V., Kaupenjohann, M., Galy, A., Schneider, B., Airo, A., Frösler, J., Davila, A.F., Arens, F.L., Cáceres, L., Cornejo, F.S., Carrizo, D., Dartnell, L., Diruggiero, J., Flury, M., Ganzert, L., Gessner, M.O., Grathwohl, P., Guan, L., Heinz, J., Hess, M., Keppler, F., Maus, D., McKay, C.P., Meckenstock, R.U., Montgomery, W., Oberlin, E.A., Probst, A.J., Sáenz, J.S., Sattler, T., Schirmack, J., Sephton, M.A., Schloter, M., Uhl, J., Valenzuela, B., Vestergaard, G., Wörmer, L., Zamorano, P., 2018. Transitory microbial habitat in the hyperarid Atacama Desert. Proc. Natl. Acad. Sci. U. S. A. 115 (11), 2670–2675. http://dx.doi.org/10.1073/pnas.1714341115.

Schwertmann, U., 1964. Differenzierung der Eisenoxide des Bodens durch Extraktion mit Ammoniumoxalat-Lösung. J. Plant Nutr. Soil Sci. 105, 194–202.

Sessitsch, A., Weilharter, A., Gerzabek, M.H., Kirchmann, H., Kandeler, E., 2001. Microbial population structures in soil particle size fractions of a long-term fertilizer field experiment. Appl. Environ. Microbiol. 67 (9), 4215–4224. http://dx.doi.org/10.1128/AEM.67.9.4215-4224.2001.

Slessarev, E.W., Lin, Y., Bingham, N.L., Johnson, J.E., Dai, Y., Schimel, J.P., Chadwick, O.A., 2016. Water balance creates a threshold in soil pH at the global scale. Nature. http://dx.doi.org/10.1038/nature20139.

Smeck, N.E., 1985. Phosphorus dynamics in soils and landscapes. Geoderma 36, 185–199. http://dx.doi.org/10.1016/0016-7061(85)90001-1.

Smith, J.L., Halvorson, J.J., Bolton, H., 2002. Soil properties and microbial activity across a 500 m elevation gradient in a semi-arid environment. Soil Biol. Biochem. 34 (11), 1749–1757. http://dx.doi.org/10.1016/S0038-0717(02)00162-1.

Sommer, M., Schlichting, E., 1997. Archetypes of catenas in respect to matter — a concept for structuring and grouping catenas. Geoderma 76 (1–2), 1–33. http://dx.doi.org/10.1016/S0016-7061(96)00095-X.

Troughton, J.H., Card, K.A., 1975. Temperature effects on the carbon-isotope ratio of C3, C 4 and crassulacean-acid-metabolism (CAM) plants. Planta 123 (2), 185–190. http://dx.doi.org/10.1007/BF00383867.

Wagner, D., Pfeiffer, E.-M., Bock, E., 1999. Methane production in aerated marshland and model soils: effects of microflora and soil texture. Soil Biol. Biochem. 31, 999–1006. http://dx.doi.org/10.1016/S0038-0717(99)00011-5.

Wang, F., Michalski, G., Luo, H., Caffee, M., 2017. Role of biological soil crusts in affecting soil evolution and salt geochemistry in hyper-arid Atacama Desert, Chile. Geoderma 307, 54–64. http://dx.doi.org/10.1016/j.geoderma.2017.07.035.

Weedon, J.T., Cornwell, W.K., Cornelissen, J.H.C., Zanne, A.E., Wirth, C., Coomes, D.A., 2009. Global meta-analysis of wood decomposition rates: a role for trait variation among tree species? Ecol. Lett. 12 (1), 45–56. http://dx.doi.org/10.1111/j.1461-0248.2008.01259.x.

Wei, T., Simko, V., 2017. R Package "Corrplot": Visualization of a Correlation Matrix (Version 0.84). Available from. https://github.com/taiyun/corrplot.

Werth, M., Kuzyakov, Y., 2010. 13C fractionation at the root–microorganisms–soil interface: a review and outlook for partitioning studies. Soil Biol. Biochem. 42 (9), 1372–1384. http://dx.doi.org/10.1016/j.soilbio.2010.04.009.

Wickham, H., 2009. GGplot2: Elegant Graphics for Data Analysis, Second edition. Springer New York, New York, NY, pp. 260.

Will, C., Thürmer, A., Wollherr, A., Nacke, H., Herold, N., Schrumpf, M., Gutknecht, J., Wubet, T., Buscot, F., Daniel, R., 2010. Horizon-specific bacterial community composition of German grassland soils, as revealed by pyrosequencing-based analysis of 16S rRNA genes. Appl. Environ. Microbiol. 76 (20), 6751–6759. http://dx.doi.org/10.1128/AEM.01063-10.

Williams, L., Borchhardt, N., Colesie, C., Baum, C., Komsic-Buchmann, K., Rippin, M., Becker, B., Karsten, U., Büdel, B., 2017. Biological soil crusts of Arctic Svalbard and of Livingston Island, Antarctica. Polar Biol. 40 (2), 399–411. http://dx.doi.org/10.1007/s00300-016-1967-1.

Wright, K., 2017. Corrgram: plot a correlogram. R package version 1.12. https://CRAN.R-project.org/package=corrgram.

Wysocki, D.A., Zanner, C.W., 2006. Landscape elements. In: Lal, R. (Ed.), Encyclopedia of Soil Science, 2nd ed. Taylor & Francis, New York, Abingdon, Oxon, pp. 1008–1012.

Xu, M., Li, X., Cai, X., Gai, J., Li, X., Christie, P., Zhang, J., 2014. Soil microbial community structure and activity along a montane elevational gradient on the Tibetan Plateau. Eur. J. Soil Biol. 64, 6–14. http://dx.doi.org/10.1016/j.ejsobi.2014.06.002.

Zhao, N., Li, X.G., 2017. Effects of aspect–vegetation complex on soil nitrogen mineralization and microbial activity on the Tibetan Plateau. Catena 155, 1–9. http://dx.doi.org/10.1016/j.catena.2017.02.025.

Zhou, J., Xia, B., Treves, D.S., Wu, L.-Y., Marsh, T.L., O'Neill, R.V., Palumbo, A.V., Tiedje, J.M., 2002. Spatial and resource factors influencing high microbial diversity in soil. Appl. Environ. Microbiol. 68 (1), 326–334.